Biogeosciences Discuss., doi:10.5194/bg-2015-627, 2016
Manuscript under review for journal Biogeosciences
Published: 18 January 2016

Biogeosciences
Discussions
Open Access

Accurate and precise quantification of atmospheric nitrate in streams draining land of various uses by using triple oxygen isotopes as tracers

Urumu Tsunogai[1], Takanori Miyauchi[1], Takuya Ohyama[1], Daisuke D. Komatsu[1,*], Fumiko Nakagawa[1], Yusuke Obata[2], Keiichi Sato[3], and Tsuyoshi Ohizumi[3]

[1]{Graduate School of Environmental Studies, Nagoya University, Furo-cho, Chikusa-ku, Nagoya 464-8601, Japan}

[2]{Faculty of Bioresources, Mie University, 1577 Kurimamachiya-cho, Tsu 514-8507, Japan}

[3]{Asia Center for Air Pollution Research, 1182 Sowa Nishi-ku, Niigata 950-2144, Japan}

[*]{now at School of Marine Science and Technology, Tokai University, 3-20-1 Orito, Shimizu, Shizuoka 424-8610, Japan}

Correspondence to: U. Tsunogai (urumu@nagoya-u.jp)

Abstract

^{17}O anomalies were used to quantify the influence of changes in land use and population density between each catchment area on the fate of atmospheric nitrate by determining the areal distribution and seasonal variation in stable isotopic compositions including the ^{17}O anomalies (Δ^{17}O) of nitrate for more than 30 streams within the same watershed. Those in precipitation (wet deposition; $n = 213$) sampled at Sado-seki monitoring station were determined for three years as well. The deposited nitrate showed similar large ^{17}O anomalies with those already reported for mid-latitudes: Δ^{17}O values ranged from +18.6‰ to +32.4‰ with a three-year average of +26.3‰. However, nitrate in each inflow stream showed small annual average Δ^{17}O values ranging from +0.5‰ to +3.1‰, which corresponds to the mixing ratios of unprocessed atmospheric nitrate to total nitrate from 1.8 ± 0.3% to 11.8 ± 1.8%, with 5.1 ± 0.5% as the average of all inflow streams. Although the annual average Δ^{17}O values

tended to be smaller in accordance with the increase in annual average nitrate concentration from 12.7 to 106.2 μmol L^{-1}, the absolute concentrations of unprocessed atmospheric nitrate in the streams were almost stable at 2.3 ± 1.1 μmol L^{-1} irrespective of the changes in population density and land use in each catchment area. We conclude that changes in population density and land use between each catchment area had little impact on the concentration of atmospheric nitrate. Thus, the total nitrate concentration originated primarily from additional contribution of remineralized nitrate from both natural sources, having values of +4.4 ± 1.8‰ and −2.3 ± 0.9‰ for $\delta^{15}N$ and $\delta^{18}O$, respectively, and anthropogenic sources having values of +9.2 ± 1.3‰ and −2.2 ± 1.1‰ for $\delta^{15}N$ and $\delta^{18}O$, respectively. In addition, both the uniform absolute concentration of atmospheric nitrate and the low and uniform $\delta^{18}O$ values of the remineralized portion of nitrate in the streams imply that in-stream removal of nitrate through assimilation or denitrification had small impact on the concentrations and stable isotopic compositions of nitrate in the streams, except for a few streams in summer having catchments of urban/suburban land uses. Additional measurements of the $\Delta^{17}O$ values of nitrate together with $\delta^{15}N$ and $\delta^{18}O$ enabled us to exclude the contribution of unprocessed atmospheric nitrate from the determined $\delta^{15}N$ and $\delta^{18}O$ values of total nitrate and to use the corrected $\delta^{15}N$ and $\delta^{18}O$ values to evaluate the source and behaviour of the remineralized portion of nitrate in each stream.

1 Introduction

Nitrate (NO_3^-) in stream water can be an important clue for understanding the biogeochemical cycles within its catchment area (Durka et al. 1994; Likens et al. 1970; Swank et al. 2001). In addition, the nitrate concentration in stream water is important to primary production and thus eutrophication downstream, including lakes, estuaries, and oceans (Mcisaac et al. 2001; Paerl 2009). Nitrate concentrations in stream water, however, are determined through a complicated interplay of several processes within its catchment area including (1) the addition of atmospheric nitrate ($NO_3^-{}_{atm}$) through deposition, (2) the production of remineralized nitrate ($NO_3^-{}_{re}$) through microbial nitrification, and (3) the removal of nitrate through assimilation and denitrification by plants and microbes. In addition to natural processes, anthropogenic processes could have a significant impact on the nitrate dynamics within each catchment area, particularly for those eluted from urban or agricultural catchment zones. Therefore, interpretation of the processes regulating nitrate concentration in stream water is not always straightforward.

The $^{15}N/^{14}N$ and $^{18}O/^{16}O$ ratios of nitrate have been widely applied in the determination of the sources and behaviours of nitrate in stream water worldwide (Barnes et al. 2008; Barnes and Raymond 2010; Burns et al. 2009; Burns and Kendall 2002; Campbell et al. 2002; Campbell et al. 2006; Costa et al. 2011; Curtis et al. 2011; Durka et al. 1994; Hales et al. 2007; Johannsen et al. 2008; Kaushal et al. 2011; Lohse et al. 2013; Mayer et al. 2002; Nestler et al. 2011; Ohte 2013; Ohte et al. 2004; Ohte et al. 2010; Pellerin et al. 2012; Silva et al. 2002; Thibodeau et al. 2013; Tobari et al. 2010; Wankel et al. 2006; Williard et al. 2001; Yue et al. 2013; Zeng and Wu 2015). By combining the two isotopic ratios, the relative mixing ratios among various nitrate sources such as atmospheric (unprocessed), fertilizer, manure, and sewage plants can be quantified through a simple isotope mass balance approach. Partial removal of nitrate through either assimilation or denitrification, however, results in residual nitrate being enriched with ^{15}N and ^{18}O (Böttcher et al. 1990; Granger et al. 2010), which complicates their interpretation beyond that of the simple isotope mass balance approach. In addition, trace contributions of unprocessed $NO_3^-{}_{atm}$ could have a significant impact on the $^{18}O/^{16}O$ ratios of the total nitrate in stream water (Durka et al. 1994; Kendall 1998; Mayer et al. 2001; Michalski et al. 2004; Tsunogai et al. 2010). Therefore, $^{18}O/^{16}O$ ratios are used as tracers based on assumptions such as (1) the $^{18}O/^{16}O$ ratios of nitrate in stream water simply reflect the mixing ratio of unprocessed $NO_3^-{}_{atm}$ within total nitrate (Barnes et al. 2008; Burns et al. 2009; Campbell et al. 2006; Durka et al. 1994; Ohte et al. 2004; Ohte et al. 2010; Zeng and Wu 2015), and (2) the mixing ratios of unprocessed $NO_3^-{}_{atm}$ within total nitrate are minimum or uniform for whole or specific stream water samples (Johannsen et al. 2008; Mayer et al. 2002; Wankel et al. 2006). To verify the reliability of these assumptions and to utilize the $^{18}O/^{16}O$ ratios for the quantification of the accurate and precise mixing ratios among various nitrate sources based on the isotope mass balance approach, the mixing ratio of $NO_3^-{}_{atm}$ within the total nitrate in stream water must be better understood; otherwise, the processes regulating nitrate concentration in stream water will be ambiguous even when adding the data of $^{18}O/^{16}O$ ratios of nitrate.

To overcome the limitation in using the $^{15}N/^{14}N$ and $^{18}O/^{16}O$ ratios, the $^{17}O/^{16}O$ ratios of nitrate have been used as an additional tracer of $NO_3^-{}_{atm}$ in stream water in recent studies (Dejwakh et al. 2012; Michalski et al. 2004; Riha et al. 2014; Rose et al. 2015; Tsunogai et al.

2010; Tsunogai et al. 2014). The $^{17}O/^{16}O$ ratios were used because, whereas $NO_3^-{}_{re}$, the oxygen atoms of which are derived from either terrestrial O_2 or H_2O through nitrification, shows mass-dependent relative variations between $^{17}O/^{16}O$ and $^{18}O/^{16}O$ ratios, unprocessed $NO_3^-{}_{atm}$ displays an anomalous enrichment in ^{17}O from the mass-dependent relative variations, reflecting oxygen atom ~~transfers~~ from ozone during the conversion of NO_x to $NO_3^-{}_{atm}$ (Michalski et al. 2003; Morin et al. 2008). By using the $\Delta^{17}O$ signature defined by the following equation (Kaiser et al. 2007; Miller 2002), we can distinguish $NO_3^-{}_{atm}$ ($\Delta^{17}O > 0$) from $NO_3^-{}_{re}$ ($\Delta^{17}O = 0$):

$$\Delta^{17}O = \frac{1+\delta^{17}O}{\left(1+\delta^{18}O\right)^{\beta}} - 1, \qquad (1)$$

where the constant β is 0.5247 (Kaiser et al. 2007; Miller 2002), $\delta^{18}O = R_{sample}/R_{standard} - 1$, and R is the $^{18}O/^{16}O$ ratio of the sample (or the $^{17}O/^{16}O$ ratio in the case of $\delta^{17}O$ or the $^{15}N/^{14}N$ ratio in the case of $\delta^{15}N$) and each standard reference material. In addition, $\Delta^{17}O$ is stable during the mass-dependent isotope fractionation processes within surface ecosystems. Therefore, although the atmospheric $\delta^{15}N$ or $\delta^{18}O$ signature can be overprinted by biogeochemical processes subsequent to deposition, $\Delta^{17}O$ can be used as a robust tracer of unprocessed $NO_3^-{}_{atm}$ to reflect the mixing ratio of unprocessed $NO_3^-{}_{atm}$ within total NO_3^- regardless of biogeochemical removal processes subsequent to deposition by using the following equation:

$$\frac{C_{atm}}{C_{total}} = \frac{\Delta^{17}O}{\Delta^{17}O_{atm}}, \qquad (2)$$

where C_{atm} and C_{total} denote the concentration of $NO_3^-{}_{atm}$ and NO_3^- in each water sample, respectively, and $\Delta^{17}O_{atm}$ and $\Delta^{17}O$ denote the $\Delta^{17}O$ values of $NO_3^-{}_{atm}$ and nitrate (total) in each water sample, respectively.

Moreover, additional measurements of the $\Delta^{17}O$ values of nitrate together with $\delta^{15}N$ and $\delta^{18}O$ enable us to exclude the contribution of $NO_3^-{}_{atm}$ in the determined $\delta^{15}N$ and $\delta^{18}O$ values and to estimate the corrected $\delta^{15}N$ and $\delta^{18}O$ values ($\delta^{15}N_{re}$ and $\delta^{18}O_{re}$, respectively) for accurate evaluation on the source and behaviour of $NO_3^-{}_{re}$ (Dejwakh et al. 2012; Liu et al. 2013; Riha et al. 2014; Tsunogai et al. 2011; Tsunogai et al. 2010; Tsunogai et al. 2014).

Previous studies have successfully applied the $\Delta^{17}O$ tracer of nitrate to those eluted from arid/semi-arid watersheds (Dejwakh et al. 2012; Michalski et al. 2004; Riha et al. 2014), forested watersheds (Rose et al. 2015; Tsunogai et al. 2010; Tsunogai et al. 2014), and a large river basin (Liu et al. 2013) to determine the accurate and precise mixing ratios of unprocessed $\mathrm{NO_3^-}_{\mathrm{atm}}$ in total nitrate in addition to the fate of the $\mathrm{NO_3^-}_{\mathrm{atm}}$ that had been deposited into each watershed. However, relative changes in the source and fate of $\mathrm{NO_3^-}_{\mathrm{atm}}$ in accordance with the changes in land use of catchments have not been studied thus far by using the Δ^{17}O tracer of nitrate.

In this study, we measure the concentrations and the stable isotopic compositions of nitrate including Δ^{17}O values for more than 30 streams flowing into a lake in Japan with catchments of widely varying land uses within the same watershed, which includes urban, suburban, agricultural (mostly rice paddies), and forested catchments. By using the Δ^{17}O tracer, we quantify both areal and temporal variations in the concentrations of both $\mathrm{NO_3^-}_{\mathrm{atm}}$ and $\mathrm{NO_3^-}_{\mathrm{re}}$ in streams across the land use settings to gain insight into the processes controlling the source, transport, and fate of $\mathrm{NO_3^-}_{\mathrm{atm}}$ and $\mathrm{NO_3^-}_{\mathrm{re}}$ (Fig. 1). ~~Although~~ $\mathrm{NO_3^-}_{\mathrm{re}}$ increases during nitrification within each catchment area, ~~for instance,~~ $\mathrm{NO_3^-}_{\mathrm{atm}}$ is stable, so that we can evaluate the progress of nitrification within each catchment area by using the changes in the concentrations of both $\mathrm{NO_3^-}_{\mathrm{atm}}$ and $\mathrm{NO_3^-}_{\mathrm{re}}$. Besides ~~to~~ the streams, we ~~determine~~ those values in precipitation (wet deposition) for comparison to obtain accurate and precise mixing ratios of both $\mathrm{NO_3^-}_{\mathrm{atm}}$ and $\mathrm{NO_3^-}_{\mathrm{re}}$ within nitrate (total) in each stream. Moreover, we exclude the contribution of $\mathrm{NO_3^-}_{\mathrm{atm}}$ in the determined δ^{15}N and δ^{18}O values to estimate the corrected δ^{15}N and δ^{18}O values for accurate evaluation of the source and behaviour of $\mathrm{NO_3^-}_{\mathrm{re}}$. Further, we determine those values in an outflow stream of the same lake to evaluate the influences of flow stagnation ~~into~~ the lake on nitrate by using the differences between inflows and outflows (Fig. 1). The results presented herein will increase our understanding of the fate of $\mathrm{NO_3^-}_{\mathrm{atm}}$ deposited onto land, particularly ~~those~~ deposited ~~onto~~ urban/suburban and forested catchments (Fig. 1).

2 Experimental Section

2.1 Site description

2.1.1 Lake Biwa watershed basin

Lake Biwa, located in the central part of the Japanese Islands, is the largest freshwater lake in Japan (Fig. 2). It has a surface area of 670.4 km^2 and a total catchment area of 3174 km^2 with annual precipitation of around 2000 mm. More than 120 streams flow into the lake, whereas the Seta River (No. 33 in Fig. 2(b)) at the southern end, also known as the Yodo River, is the only natural outflow. The average residence time of water in the lake is 5.5 years.

Similar to many lakes throughout the world, Lake Biwa has experienced eutrophication in the past. Urbanization near the lake beginning in the 1960s, particularly on the southern and eastern shore, likely caused an increase in nutrient loading. Blooms of *Uroglena americana* and cyanobacteria have occurred since 1977 and 1983, respectively (Hsieh et al. 2011). To clarify the pathways and sources of nitrate that were fed into the lake, the stable isotopic compositions (δ^{15}N and δ^{18}O) of dissolved nitrate were determined in the major streams flowing into the lake (Ohte et al. 2010). Based on the δ^{15}N values of nitrate showing positive correlation with population densities of each catchment area, it was concluded that sewage effluent was the dominant source contributing to the increase in the δ^{15}N values of nitrate.

2.1.2 Sado-seki monitoring station

Sado-seki National Acid Rain Monitoring Station (38°14′59″N, 138°24′00″E) was established on Sado Island (Fig. 2(a)), at 110 m above sea level, as a monitoring observatory of the Acid Deposition Monitoring Network in East Asia (EANET) representing the central Japan area (EANET 2014). The monitoring has shown that the observatory received 24.5 mmol NO_3^- $m^{-2}yr^{-1}$ and 17.1 mmol NH_4^+ $m^{-2}yr^{-1}$ on average from ~~FY~~2009 to 2011 (EANET 2014), which corresponds to a total ~~fixed~~ N deposition rate of 5.8 kg of N $ha^{-1}yr^{-1}$.

2.2 Sampling

Stream water samples were collected near the mouths of each stream during base flow periods four times in 2013 on March 15, June 17, August 5, and October 21 from 33 inflow streams and 1 outflow river (Seta River) of Lake Biwa (Table 1; Fig. 2(b)) except for stream Nos. 3 and 28 in June, which became dry arroyos at that time. The catchments of the studied inflow streams occupied 70% of the entire Lake Biwa basin area. The streams were selected to cover those in which the concentrations and stable isotope compositions of nitrate, δ^{15}N and δ^{18}O, had already been determined in 2004–2006 (Ohte et al. 2010). The categories of locations classified by Ohte et al. (2010) were also used in this study to classify the location of the streams (Table 1). Either a bucket or dipper was used to collect samples as far from the bank as possible. Each sample was transferred into a dark polyethylene bottle that was pre-rinsed at least twice with the sample itself and stored ~~under refrigeration~~. Then, the samples were filtered through a pre-combusted Whatman GF/F filter with a 0.7 μm pore size within a few hours after collection, and the filtrate was stored in a different dark polyethylene bottle ~~under refrigeration~~ at 4°C until analysis.

To calculate the annual influx/efflux of nitrate via each stream to/from Lake Biwa as well as its seasonal variation, we used the sampling number n, where n = 1, 2, 3, and 4, ~~to represent~~ the sampling in March, June, August, and October, respectively. In addition, we used one more hypothetical sampling number (n = 5) set just one year later than the n = 1 date to quantify the annual influx/efflux. Accordingly, we assumed that secular change was minimum in the streams and that the streams returned back to the initial state one year later. Furthermore, we rated the interval between n = 1 and 2 as spring, n = 2 and 3 as summer, n = 3 and 4 as autumn, and n = 4 and 5 as winter for the streams in this study.

Samples of wet deposition were taken at the Sado-seki National Acid Rain Monitoring Station by using standard methods for evaluating acid deposition in Japan from April 2009 to March 2012. An automatic wet deposition sampler (US-420, Ogasawara) was used in the collection. All of the deposition samples were ~~introduced and~~ stored in 1 L polyethylene bottles ~~under refrigeration~~ until daily recovery. After measuring both the conductivity and pH, the recovered samples were filtered through a 0.2 μm pore-size membrane filter (Dismic-25CS, ADVANTEC) and stored in a refrigerator until analysis. The annual wet deposition rate of nitrate was 19.3 mmol $m^{-2}y^{-1}$ for FY2009, from April 2009 to March 2010; 28.0 mmol $m^{-2}y^{-1}$ for FY2010, from April 2010 to March 2011; and 27.0 mmol $m^{-2}y^{-1}$ for FY2011, from April 2011 to March 2012 (EANET 2014).

2.3 Analysis

The concentrations of nitrate (NO_3^-) and nitrite (NO_2^-) in each filtrate sample were measured by ion chromatography (Prominence HIC-SP, Shimadzu, Japan) within a few days after each sampling. The $\delta^{18}O$ values of H_2O in the samples were analysed by using the cavity ring-down spectroscopy method by employing the Picarro L2120-I instrument equipped with an A0211 vaporizer and auto sampler; the error in this method was ±0.1‰. Both Vienna

Standard Mean Ocean Water (VSMOW) and Standard Light Antarctic Precipitation (SLAP) were used to calibrate the values to the international scale.

To determine the stable isotopic compositions, nitrate in each filtrate sample was chemically converted to N_2O by using a method originally developed to determine the $^{15}N/^{14}N$ and $^{18}O/^{16}O$ ratios of seawater and freshwater nitrate (Mcilvin and Altabet 2005) which was later modified (Konno et al. 2010; Nakagawa et al. 2013; Tsunogai et al. 2011; Tsunogai et al. 2008; Tsunogai et al. 2010; Yamazaki et al. 2011). Then, the stable isotopic compositions of N_2O were determined by using a continuous-flow isotope ratio mass spectrometry (CF-IRMS) system in Nagoya University (Hirota et al. 2010; Komatsu et al. 2008). The analytical procedures are the same as those detailed in previous research (Nakagawa et al. 2013; Tsunogai et al. 2014).

To determine whether samples were deteriorated or contaminated during storage and whether the conversion rate from nitrate to N_2O was sufficient, concentrations of nitrate in the samples were determined each time we analysed isotopic compositions using MS based on the N_2O^+ or O_2^+ outputs. We adopted the $\delta^{15}N$, $\delta^{18}O$, or $\Delta^{17}O$ values only when concentrations measured by MS correlated with those measured by ion chromatography just after the sampling within 10% differences.

We repeated the analyses on the $\delta^{15}N$, $\delta^{18}O$, and $\Delta^{17}O$ values of nitrate at least three times for each sample to attain high precision. Most of the samples had nitrate concentrations of more than 5.0 μmol L^{-1}, which corresponded to nitrate quantities greater than 50 nmol in a 10 mL sample. This amount was sufficient for determining the $\delta^{15}N$, $\delta^{18}O$, and $\Delta^{17}O$ values with high precision. The sample volume was increased to 30 mL for ~~those having~~ nitrate concentrations less than 5.0 μmol L^{-1}; the number of analyses was also increased in such cases. Thus, all isotopic data presented in this study have an error better than ±0.2‰ for $\delta^{15}N$, ±0.3‰ for $\delta^{18}O$, and ±0.1‰ for $\Delta^{17}O$.

Because the more precise power law shown in Eq. (1) was used to calculate $\Delta^{17}O$, the estimated $\Delta^{17}O$ values were somewhat different from those estimated based on traditional linear approximation (Michalski et al. 2002). Please note that our $\Delta^{17}O$ values of $NO_3^-{}_{\mathrm{atm}}$ would be 0.9±0.1 ‰ higher if we ~~use~~ the linear approximation. However, these differences were insignificant for most of the stream water samples evaluated in this study.

Nitrite (NO_2^-) in the samples interferes with the final N_2O produced from nitrate (NO_3^-) because the chemical method also converts NO_2^- to N_2O (Mcilvin and Altabet 2005).

Therefore, it is sometimes necessary to correct for the contribution of NO_2^--derived N_2O to accurately determine the stable isotopic compositions of the sample nitrate. However, all samples analysed for stable isotopic compositions in this study showed NO_2^-/NO_3^- ratios of less than 5%; thus, the results were used with no corrections.

2.4 Calculating average concentration and isotopic compositions in each stream

To quantitatively clarify the chemical and isotopic characteristics of each stream, we determined both the flow-weighted annual average concentration ($\bar{C}_{total}$) and flow-weighted annual average $\delta^{15}N$, $\delta^{18}O$, and $\Delta^{17}O$ values ($\bar{\delta}$) of nitrate for each stream by using Eqs. (3), (4), and (5):

$$q = \sum_{n=1}^{4} \left(f_n \cdot \Delta t_n \right), \tag{3}$$

$$\bar{C}_{total} = \frac{\sum_{n=1}^{4} \left(C_n \cdot f_n \cdot \Delta t_n \right)}{q}, \tag{4}$$

$$\bar{\delta} = \frac{\sum_{n=1}^{4} \left(\delta_n \cdot C_n \cdot f_n \cdot \Delta t_n \right)}{\sum_{n=1}^{4} \left(C_n \cdot f_n \cdot \Delta t_n \right)}, \tag{5}$$

where C_n and δ_n denote the concentration (C_{total} in Eq. (2)) and isotopic values ($\delta^{15}N$, $\delta^{18}O$, or $\Delta^{17}O$) of nitrate in each stream during each observation n, respectively; f_n denotes the flow rate of each stream during each observation n; and Δt_n denotes the time interval between the observation n and the next observation n+1. When possible, we used the flow rate of each stream which was determined monthly by the Shiga Prefecture (Shiga_Prefecture 2015) for f_n. For small streams with no data for the flow rate, we used a small and stable flow rate of 0.1 m^3/s for f_n.

2.5 Calculating $\delta^{15}N$ and $\delta^{18}O$ of remineralized nitrate

To exclude the contribution of $NO_3^-{}_{atm}$ from the $\delta^{15}N$ and $\delta^{18}O$ values of nitrate and to clarify the source and behaviour of $NO_3^-{}_{re}$ by using both $\delta^{15}N$ and $\delta^{18}O$ as tracers, we estimated the end-member $\delta^{15}N$ and $\delta^{18}O$ values of the remineralized nitrate portion, $\delta^{15}N_{re}$ and $\delta^{18}O_{re}$, by excluding the contribution of $NO_3^-{}_{atm}$ in each nitrate (Dejwakh et al. 2012; Liu et al. 2013; Riha et al. 2014; Tsunogai et al. 2011; Tsunogai et al. 2010; Tsunogai et al. 2014) by using Eqs. (6) and (7):

$$\delta^{15}N_{re} = \frac{C_{total} \cdot \delta^{15}N - C_{atm} \cdot \delta^{15}N_{atm}}{C_{total} - C_{atm}}, \tag{6}$$

$$\delta^{18}O_{re} = \frac{C_{total} \cdot \delta^{18}O - C_{atm} \cdot \delta^{18}O_{atm}}{C_{total} - C_{atm}}, \tag{7}$$

where C_{atm} and C_{total} denote the concentration of $NO_3^-{}_{atm}$ and nitrate in each water sample, respectively, and $\delta^{15}N_{atm}$, $\delta^{18}O_{atm}$, and $\Delta^{17}O_{atm}$ denote the $\delta^{15}N$, $\delta^{18}O$, and $\Delta^{17}O$ values of $NO_3^-{}_{atm}$ in each sample, respectively. The actual values of $\delta^{15}N_{atm}$, $\delta^{18}O_{atm}$, and $\Delta^{17}O_{atm}$ used in this study will be determined in section 3.1.

3 Results and Discussion

3.1 Atmospheric Nitrate

The triple oxygen isotopic compositions ($\Delta^{17}O$) of atmospheric nitrate ($NO_3^-{}_{atm}$) are plotted in Fig. 3(c) as a function of the sampling day (local time, UT +9:00), together with the $\delta^{15}N$ and $\delta^{18}O$ of $NO_3^-{}_{atm}$ in Figs. 3(a) and 3(b). The atmospheric nitrate at Sado-seki monitoring station showed large ^{17}O anomalies with $\Delta^{17}O$ values from +18.6‰ to +32.4‰.

Moreover, a clear normal correlation with $\delta^{18}O$ was shown (Supplement Fig. S1). A similar trend has been reported in atmospheric nitrate aerosols collected for a one-year period in La Jolla, California (32.7°N, 117.2°W) (Michalski et al. 2003), and in other areas worldwide (Kaiser et al. 2007; Morin et al. 2009). Michalski et al. (2003) interpreted that the linear correlation corresponds to the mixing line between the tropospheric ozone and tropospheric H_2O, and thus tropospheric OH radicals, with $\Delta^{17}O = 0‰$ and $\delta^{18}O = –5‰$. The $NO_3^-{}_{atm}$ data obtained at Sado-seki monitoring station, however, showed a somewhat different trend in the $\Delta^{17}O$–$\delta^{18}O$ plot between summer, from May to October, and winter, from November to April (Supplement Fig. S1). Although the linearly fitted line to the summer data showed a slope of 2.21 ± 0.22 and an intercept of +19.7 ± 5.1‰ in the $\Delta^{17}O$–$\delta^{18}O$ plot, that to the winter data showed a statistically significant larger slope of 2.89 ± 0.38 and the smaller intercept of +3.0 ± 9.2‰; all errors were in the 2 σ range. Although the winter data included an intercept of

−5‰ as the end member $\delta^{18}O$ value of the tropospheric OH radical within the possible error range, as reported by Michalski et al. (2003), the intercept of summer data deviated strongly from the value. Because the monitoring station is located in the Asian monsoon area, the major air mass that arrived at the station was seasonally different; Pacific air originated from the south-eastern direction in summer whereas continental air originated from north-western direction in winter. The present results imply seasonal and regional changes in the $\delta^{18}O/\Delta^{17}O$ ratios of tropospheric ozone and in the OH radical.

On the basis of both the temporal variation in the depositional flux of $NO_3^-{}_{atm}$ and the $\Delta^{17}O$ value, we estimated the average $\Delta^{17}O$ value of $NO_3^-{}_{atm}$ ($\Delta^{17}O_{avg}$) deposited at Sado-seki monitoring station as +25.5‰ for FY2009, +27.2‰ for FY2010, +25.7‰ for FY2011, and +26.3‰ for the three years by using

$$\Delta^{17}O_{avg} = \frac{\sum_k \left(C_k \cdot V_k \cdot \Delta^{17}O_k\right)}{\sum_k \left(C_k \cdot V_k\right)}, \tag{8}$$

where C_k denotes the concentration of nitrate in each wet deposition sample, and V_k denotes the total water volume of each wet deposition sample. Substituting $\Delta^{17}O$ with $\delta^{15}N$ ($\delta^{18}O$) in Eq. (8), we estimated $\delta^{15}N_{avg}$ ($\delta^{18}O_{avg}$) as −4.4 ‰ (+78.5‰) for FY2009, −3.8 ‰ (+81.8‰) for FY2010, −4.4 ‰ (+78.6‰) for FY2011, and −4.2‰ (+79.8‰) for the three years.

To apply the $\Delta^{17}O_{avg}$ values obtained at Sado-seki monitoring station as ~~for~~ $\Delta^{17}O$ of $NO_3^-{}_{atm}$ deposited ~~into~~ the studied watershed (i.e. $\Delta^{17}O_{atm}$ in Eq. (2)), however, additional corrections could be needed because the $\Delta^{17}O$ value of $NO_3^-{}_{atm}$ is a function of the NO_x oxidation channels in the atmosphere that shift depending on the intensity of sunlight, temperature, and oxidant levels (e.g. Alexander et al. 2009; Kunasek et al. 2008; Michalski et al. 2003; Morin et al. 2012; Morin et al. 2008; Savarino et al. 2013). The latitudinal difference between Sado-seki monitoring station (38°15′N, 138°24′E; Fig. 2) and the watershed studied (35°15′N, 136°5′E; Fig. 2) could change the intensity of sunlight and thus the NO_x oxidation channel. Moreover, Tsunogai et al. (2010) reported that nitrate in polluted air masses derived directly from megacities in winter showed slightly larger $\Delta^{17}O$ values than those in the same seasons owing likely to the relative increase in the reaction via NO_3 radicals within the entire $NO_3^-{}_{atm}$ production channel to produce $NO_3^-{}_{atm}$ in the polluted air mass. The annual average $\Delta^{17}O$ ~~values~~ determined in this study was ~~the~~ lowest ~~value~~ in FY2009 when the deposition rate was the smallest, at 19.3 mmol $m^{-2}y^{-1}$ (EANET 2014), whereas the annual average $\Delta^{17}O$ value was ~~the~~ highest ~~value~~ in FY2010 when the deposition rate was the largest, at 28.0 mmol $m^{-2}y^{-1}$ for nitrate, within the three years of observation. These results also imply that ~~we must correct for~~ the difference in arrival frequency of polluted air ~~mass as well.~~

Nevertheless, both the annual average and the seasonal variation range of $\Delta^{17}O$ correlated strongly with those determined at Rishiri monitoring station (45°07′11″N, 141°12′33″E) in FY2008, at +26.2‰ (Tsunogai et al. 2010), where the wet deposition rate of $NO_3^{-}{}_{atm}$ was an average 40% smaller that at Sado-seki monitoring station from 2000 to 2013 (EANET 2014). Moreover, the values also coincided with those reported for mid-latitudes, such as at La Jolla, at 33°N (Michalski et al. 2003) and Princeton, at 40°N (Kaiser et al. 2007). We concluded that by allowing an appropriate range of errors presented later, the obtained $\Delta^{17}O_{avg}$ value of $NO_3^{-}{}_{atm}$ can ~~represent those deposited at middle~~ latitudes worldwide, including the Lake Biwa watershed basin.

In addition, the actual $\Delta^{17}O_{atm}$ values of $NO_3^{-}{}_{atm}$ in each stream water sample can differ from the $\Delta^{17}O_{avg}$ owing to the seasonal variation in the $\Delta^{17}O$ values of $NO_3^{-}{}_{atm}$. In correcting for the seasonal variation, however, it is not adequate to use the $\Delta^{17}O$ values determined for the seasons of sampling, as $\Delta^{17}O_{atm}$ in Eq. (2), because the duration of the recession period is longer than a few months for most of the forest catchments in Japan with a humid temperate climate (Ohte et al. 2010; Takimoto et al. 1994). That is, nitrate in base flow stream water had been stored in subsurface runoff and groundwater, of which seasonal $\Delta^{17}O$ changes have not been found thus far (Nakagawa et al. 2013; Tsunogai et al. 2010).

In summary, we used the obtained $\Delta^{17}O_{avg}$ value of $NO_3^{-}{}_{atm}$ as $\Delta^{17}O_{atm}$ in Eq. (2) to estimate C_{atm} in the streams of the Lake Biwa watershed basin by allowing the error range of 3.0‰, considering the whole factor change of $\Delta^{17}O_{atm}$ from $\Delta^{17}O_{avg}$. About 65% of the all $\Delta^{17}O$ data of $NO_3^{-}{}_{atm}$ obtained at Sado-seki monitoring station were included in this range of +26.3 ± 3.0‰.

In the case of $\delta^{15}N$ and $\delta^{18}O$, the values of $NO_3^{-}{}_{atm}$ in each stream water sample (i.e. $\delta^{15}N_{atm}$ and $\delta^{18}O_{atm}$ in Eqs. (6) and (7)) differed further from $\delta^{15}N_{avg}$ and $\delta^{18}O_{avg}$ owing to isotopic fractionation during partial removal subsequent to deposition. As a result, while using the $\delta^{15}N_{avg}$ and $\delta^{18}O_{avg}$ values as $\delta^{15}N_{atm}$ and $\delta^{18}O_{atm}$, we assumed much larger error range on the values; i.e. ± 10‰ for both $\delta^{15}N$ and $\delta^{18}O$. We will further discuss the appropriateness of these error ranges section 3.3. Because of the small C_{atm}/C_{total} ratios of stream water at generally less than 7% (section 3.2), the error propagated to $\delta^{15}N_{re}$ and $\delta^{18}O_{re}$ was generally small, less than 1‰ and 2‰, respectively, for most of the data presented in this study.

3.2 Stream nitrate overview

The concentrations (C_{total}) and $\delta^{15}N$, $\delta^{18}O$, and $\Delta^{17}O$ values of nitrate in the stream water samples determined for each observation (n = 1 2, 3, and 4) are presented in Fig. 4. The annual average concentration ($\overline{C}_{total}$) and annual average $\delta^{15}N$, $\delta^{18}O$, and $\Delta^{17}O$ values ($\overline{\delta^{15}N}$, $\overline{\delta^{18}O}$, and $\overline{\Delta^{17}O}$, respectively) in each stream estimated by using Eqs. (3), (4), and (5) are shown in the figure as black bars. In this figure, each stream was plotted on the x-axis in the order of location beginning from stream No. 31, which lies southwest of all of the streams (Fig. 2), and proceeding in a clockwise direction. The spatially continuous variation in the values of $\overline{\delta^{15}N}$, $\overline{\delta^{18}O}$, and $\overline{\Delta^{17}O}$ imply that the values may represent land use changes in each catchment area.

Although the $\Delta^{17}O$ values presented significant ~~areal~~ and temporal variation from +0.0‰ to +6.8‰, the range of the $\overline{\Delta^{17}O}$ values from +0.5‰ to +3.1‰ was typical for nitrate in natural stream water (Liu et al. 2013; Michalski et al. 2004; Rose et al. 2015; Tsunogai et al. 2010; Tsunogai et al. 2014). These results correspond to the mixing ratios of unprocessed $NO_3^-{}_{atm}$ to total nitrate from 1.8 ± 0.3% to 11.8 ± 1.3%, obtained by using Eq. (2).

By using the concentration (C_{total}) and $\delta^{15}N$, $\delta^{18}O$, and $\Delta^{17}O$ values of nitrate, the $NO_3^-{}_{atm}$ concentration (C_{atm}) and the $\delta^{15}N$ and $\delta^{18}O$ values of the remineralized portion of nitrate ($\delta^{15}N_{re}$ and $\delta^{18}O_{re}$) in the samples were calculated by using Eqs. (2), (6), and (7) and are plotted in Fig. 5. In addition, the annual average concentration of $NO_3^-{}_{atm}$ ($\overline{C}_{atm}$) and annual average values of $\delta^{15}N_{re}$ and $\delta^{18}O_{re}$ ($\overline{\delta^{15}N_{re}}$ and $\overline{\delta^{18}O_{re}}$, respectively) in stream nitrate were calculated and are presented in Fig. 5 as black bars. Because of the large $\delta^{18}O$ differences of about 80‰ between nitrate in streams and $NO_3^-{}_{atm}$, the $\delta^{18}O_{re}$ values were a few ‰ lower than each original $\delta^{18}O$ value in total nitrate. On the contrary, owing to the small $\delta^{15}N$ differences of less than 15‰ between the total nitrate in streams and $NO_3^-{}_{atm}$, as well as the small C_{atm}/C_{total} ratios in the streams, most of the $\delta^{15}N_{re}$ values showed small deviations of less than 1‰ from each original $\delta^{15}N$ value in the total nitrate in most of the streams.

To verify possible secular changes, the estimated $\overline{C}_{total}$, $\overline{\delta^{15}N}$, and $\overline{\delta^{18}O}$ for each stream were compared with those determined by Ohte et al. (2010) in which annual average concentration and annual average $\delta^{15}N$ and $\delta^{18}O$ values of nitrate (total) were determined for the same streams in 2004 to 2006 (Supplement Fig. S2). Although both concentrations and $\delta^{15}N$ and $\delta^{18}O$ values in the streams showed significant ~~areal~~ and temporal variations during 2013, as presented in Fig. 4, the annual average values almost correlated with the values determined in 2004 to 2006. We concluded that secular changes were minimal for nitrate in the streams, at least for the most recent 10-year period of observations.

3.3 Relationship between $\Delta^{17}O$ and $\delta^{18}O$

One of the features in the ~~areal~~ variation shown in Fig. 4 is the positive correlation between $\Delta^{17}O$ and $\delta^{18}O$. As clearly ~~presented in~~ the relationship between $\overline{\Delta^{17}O}$ and $\overline{\delta^{18}O}$ (Fig. 6), these values showed linear correlation with the r^2 value of 0.88. Because $NO_3^-{}_{atm}$ is characterized by highly elevated values of both $\Delta^{17}O$ and $\delta^{18}O$ (Fig. 3), changes in the mixing ratio of unprocessed $NO_3^-{}_{atm}$ within the total nitrate pool must be ~~strongly~~ responsible for the positive correlation between $\overline{\Delta^{17}O}$ and $\overline{\delta^{18}O}$ for nitrate in the streams.

The slope value of the least–squares-fitted line between $\overline{\Delta^{17}O}$ and $\overline{\delta^{18}O}$ (Fig. 6) also supports this hypothesis. By extrapolating the least–square-fitted line to the region of $NO_3^-{}_{atm}$ having a $\Delta^{17}O$ value of +26.3‰, we obtained $\delta^{18}O$ = +86 ± 7‰, which also corresponds with the average $\delta^{18}O$ value of $NO_3^-{}_{atm}$ of +79.8‰ obtained in section 3.1. We concluded that $\overline{\delta^{18}O}$ values primarily reflect the mixing ratio of $NO_3^-{}_{atm}$ within nitrate as well.

By extrapolating the linear correlation between $\overline{\Delta^{17}O}$ and $\overline{\delta^{18}O}$ to $\overline{\Delta^{17}O} = 0‰$, we obtained the $\delta^{18}O$ value of −2.9 ± 1.2‰ as the average $\delta^{18}O$ value of the remineralized portion of nitrate ($NO_3^-{}_{re}$) in the streams. Although the $\delta^{18}O$ value was substantially ^{18}O-depleted compared with that obtained through in vitro incubation experiments in past studies (Burns and Kendall 2002; Mayer et al. 2001; Spoelstra et al. 2007), it correlated strongly with the $\delta^{18}O$ value of $NO_3^-{}_{re}$ determined recently by using the linear relationship between $\Delta^{17}O$ and $\delta^{18}O$. This correlation occurred in the groundwater of cool-temperate forested watersheds at −4.2 ± 2.4‰, where the $\delta^{18}O(H_2O)$ was around −13‰ (Tsunogai et al. 2010) and in stream water in a cool-temperate forested watershed at −3.6 ± 0.7‰, where the $\delta^{18}O(H_2O)$ was around −11‰ (Tsunogai et al. 2014). Moreover, the $\delta^{18}O$ value of $NO_3^-{}_{re}$ obtained in this study, −2.9 ± 1.2‰, is close to the possible lowermost $\delta^{18}O$ value of $NO_3^-{}_{re}$ produced through nitrification under H_2O of −7.8 ± 1.0‰ (Buchwald et al. 2012). Furthermore, the $\delta^{18}O$ value of $NO_3^-{}_{re}$

correlates strongly with that obtained through in vitro incubation experiments in recent studies that simulated temperate forest soils (Fang et al. 2012). We concluded that the δ^{18}O value of $NO_3^-{}_{re}$ produced through nitrification in the temperate watershed having $\delta^{18}O(H_2O)$ values of −7.8 ± 1.0‰ was −2.9 ± 1.2‰ and that we should use such a low δ^{18}O value as for that produced through nitrification in the watershed. Understanding the relationship between Δ^{17}O and δ^{18}O of nitrate shown in Fig. 6 is highly useful for determining the δ^{18}O value of $NO_3^-{}_{re}$ in each watershed (Tsunogai et al. 2010).

Although the Δ^{17}O values of nitrate were stable during the biogeochemical processing such as partial removal through assimilation or denitrification, the δ^{18}O values of nitrate could vary through the isotopic fractionation processes within each catchment area. Nevertheless, the $\overline{\delta^{18}O}$ values of nitrate in the streams were plotted on the mixing line between the $NO_3^-{}_{atm}$ that had been deposited into the watershed and $NO_3^-{}_{re}$ having δ^{18}O and Δ^{17}O values close to those produced through nitrification in the catchments. We concluded that the range of isotopic fractionations owing to partial removal through assimilation or denitrification subsequent to deposition of $NO_3^-{}_{atm}$ or production of $NO_3^-{}_{re}$ within each catchment area was generally small for the major portion of nitrate eluted from the watershed. This result also supports our assumption in section 3.1 such that the actual δ^{15}N and δ^{18}O values of $NO_3^-{}_{atm}$ in each stream water sample ($\delta^{15}N_{atm}$ and $\delta^{18}O_{atm}$ in Eqs. (6) and (7)) correlate with the $\delta^{15}N_{avg}$ and $\delta^{18}O_{avg}$ estimated at Sado-seki monitoring station within an error of ±10‰.

3.4 δ^{15}N values of remineralized nitrate in streams

To trace the source of the ^{18}O-depleted $NO_3^-{}_{re}$ eluted from the watershed into the lake, the annual average δ^{15}N values of the remineralized portion of nitrate ($\overline{\delta^{15}N_{re}}$) in each inflow stream were estimated and are plotted as a function of population density in Fig. 7(c), together with $\overline{\delta^{18}O_{re}}$ and $\overline{\delta^{18}O}$ in Fig. 7(d). Although the annual average $\overline{\delta^{18}O_{re}}$ values were low and almost uniform from −4.0‰ to −0.1‰, as implied in the linear correlation between $\overline{\Delta^{17}O}$ and $\overline{\delta^{18}O}$ in Fig. 6, $\overline{\delta^{15}N_{re}}$ showed larger variation from +1.7‰ to +10.9‰. Moreover, $\overline{\delta^{15}N_{re}}$ showed positive correlation with the population density (Fig. 7). A similar trend was reported for the δ^{15}N values of total nitrate in past studies in this watershed (Ohte et al. 2010) and others (Mayer et al. 2002). We further verified that the remineralized portion of nitrate ($NO_3^-{}_{re}$) was responsible for the positive correlation between the δ^{15}N values of total nitrate and population density.

Both the concentrations and the isotopic compositions shown in Fig. 7 clearly demonstrate that most portions of the nitrate eluted from the catchments with lower population densities of less than 100 km^{-2} were produced through nitrification in naturally occurring soil organic matter (Kendall et al. 1995; Ohte et al. 2010), showing δ^{15}N values of +4.4 ± 1.8‰ and δ^{18}O values of about −2.3 ± 0.9‰. In this section, we discuss the source of the ^{15}N-enriched $NO_3^{-}{}_{re}$ eluted from the catchments with higher population densities of more than 1000 km^{-2}, showing δ^{15}N values of +9.2 ± 1.3‰ or more and δ^{18}O values of about −2.2 ± 1.1‰.

Denitrification in riverbed sediments adjacent to riparian zones or groundwater bodies (Mcmahon and Böhlke 1996) can increase the δ^{15}N value of stream nitrate. However, if such post-production alternation were responsible for the ^{15}N enrichment of $NO_3^{-}{}_{re}$ and thus the total nitrate, the values of $\delta^{18}O_{re}$ in addition to those of $\delta^{15}N_{re}$ should increase (Granger et al. 2008). Moreover, the absolute concentration of $NO_3^{-}{}_{atm}$ (C_{atm}) should decrease in accordance with the progress of denitrification. The low and uniform $\delta^{18}O_{re}$ values (Fig. 7(d)) as well as the uniform C_{atm} irrespective of the population densities (Fig. 7(b)) imply that the denitrification in riverbed sediments was minor for nitrate in the streams. Rather, the $NO_3^{-}{}_{re}$ must be enriched in ^{15}N from its initial production through nitrification within the catchments with high population densities. In addition, the small differences in δ^{18}O values of $NO_3^{-}{}_{re}$ between those values irrespective of the population densities in the catchment area (Fig. 7) imply that the essential parameters for determining the δ^{18}O values of nitrate during nitrification, such as the δ^{18}O values of H_2O and pH of soils (Buchwald et al. 2012; Fang et al. 2012), should be similar ~~between~~ them.

Based on the δ^{15}N values of total nitrate eluted from catchments with high population densities, as well as the positive correlation between the δ^{15}N values of total nitrate and population densities, Ohte et al. (2010) proposed sewage effluent as the dominant source contributing to the increase in the δ^{15}N values of total nitrate eluted from such catchments. The δ^{15}N and δ^{18}O values of $NO_3^{-}{}_{re}$ newly estimated in this study, +9.2 ± 1.3‰ or more and −2.2 ± 1.1‰, respectively, also imply that the dominant source contributing to the increase in the δ^{15}N values of total nitrate had been produced through nitrification in which the source N of the nitrate had already been enriched in ^{15}N. Although the δ^{15}N and δ^{18}O values of $NO_3^{-}{}_{re}$ eluted from the high population density catchments, $\delta^{15}N_{re}$ = +9.2 ± 1.3‰ and $\delta^{18}O_{re}$ = −2.2 ± 1.1‰, were a few ‰ lower than the δ^{15}N and δ^{18}O values of total nitrate in the sewage effluent determined in past studies (Aravena et al. 1993; Wankel et al. 2006; Widory et al.

2005; Xue et al. 2009), the slight deviations in the reported $\delta^{15}N$ and $\delta^{18}O$ values from our results can be explained by the following factors: (1) a slight contribution of $NO_3^-{}_{atm}$, and (2) the progress of denitrification subsequent to production. We concluded that sewage effluent was the most probable pollution source of nitrate to explain the observed concentrations and isotopic compositions of nitrate eluted from the catchments with high population densities, particularly for those more than 1000 ~~km^{-2}~~.

3.5 Seasonal variation

Although the annual average values of $\Delta^{17}O$ and $\delta^{18}O$ in each river, $\overline{\Delta^{17}O}$ and $\overline{\delta^{18}O}$, respectively, showed linear correlation as presented in Fig. 6, the same results were not always attained for those in each season. Particularly for those obtained during June and August (i.e. summer), some of the streams showed significant deviations in $\delta^{18}O$ of more than 5‰ from the hypothetical mixing line between $NO_3^-{}_{atm}$ ($\Delta^{17}O = +26.3$ ‰ and $\delta^{18}O = 79.8$ ‰) and $NO_3^-{}_{re}$ ($\Delta^{17}O = 0$ ‰ and $\delta^{18}O = -2.9$ ‰; Fig. 6). Even though the values of $\Delta^{17}O$ and $\delta^{18}O$ of $NO_3^-{}_{atm}$ showed seasonal variation, as presented in Fig. 3, it could not explain the large deviations from the mixing line based on the seasonal changes in $NO_3^-{}_{atm}$. Rather, we must assume some seasonal changes in the biogeochemical nitrogen cycles within each catchment area to explain the relationship because different from that of the $\Delta^{17}O$ values, the $\delta^{18}O$ values of nitrate can vary during biogeochemical processing within each catchment area. As a result, we can evaluate the seasonal changes in the biogeochemical processing within each catchment area by using the seasonal changes in the relationship between $\Delta^{17}O$ and $\delta^{18}O$ shown in Fig. 8.

The increases in the number of data plotted on the highly ^{18}O-enriched region of more than a few ‰ in $\delta^{18}O$ from the lines imply that partial nitrate removal through assimilation or denitrification was active within each catchment area in June and August. The ~~areal~~ differences in the ^{18}O enrichment also support this hypothesis. As presented in Fig. 8, ^{18}O ~~enrichments were~~ common in samples obtained at the southern streams having high population densities in each catchment area, as shown in the figure by white squares. We can ~~anticipate~~ elevated loading of both nutrients and organic matter of anthropogenic origin in these catchments, both of which naturally enhance both assimilation and denitrification.

On the contrary, most samples obtained during March and October were distributed on the hypothetical mixing line between $NO_3^-{}_{atm}$ and $NO_3^-{}_{re}$ as presented in Fig. 8. We concluded that in winter, the range of isotopic fractionation subsequent to production, such as partial removal through assimilation or denitrification, was generally small for the major portion of nitrate eluted from the watershed and fed into the lake. Therefore, the annual average values (i.e. $\overline{\delta^{18}\mathrm{O}}$ and $\overline{\Delta^{17}\mathrm{O}}$) of streams were distributed on the hypothetical mixing line, as shown in Fig. 6, because the nitrate influx in winter occupied a major portion of the annual nitrate influx. Active removal of nitrate from the streams through denitrification/assimilation in summer was also responsible for the small relative importance of nitrate influx into the lake in summer. In conclusion, the relationship between Δ^{17}O and δ^{18}O of nitrate eluted from a catchment area is a useful indicator for evaluating the biogeochemical processing within the catchment area, including the seasonal change.

3.6 ~~Areal~~ and temporal Δ^{17}O variation

By using the δ^{18}O values of nitrate as tracers, Ohte et al. (2010) found that the mixing ratios of unprocessed $\mathrm{NO_3^-}_{\mathrm{atm}}$ within the total nitrate pool were high in the northern streams of the watershed in winter, from November to late April. Our present results further verified the past results shown in Fig. 4, which adds more robust evidence through the use of the Δ^{17}O tracer for $\mathrm{NO_3^-}_{\mathrm{atm}}$.

Based on the high accumulation rate of snow in the catchment zones of the northern streams, Ohte et al. (2010) concluded that high loading of unprocessed $\mathrm{NO_3^-}_{\mathrm{atm}}$ via snow in the catchment zones increased the stored unprocessed $\mathrm{NO_3^-}_{\mathrm{atm}}$ in the snowpack, which was subsequently released into the streams during the melting seasons. This process enhanced the mixing ratio of unprocessed $\mathrm{NO_3^-}_{\mathrm{atm}}$ within the total nitrate pool during the melting season, which was also reported for streams worldwide (Kendall et al. 1995; Ohte et al. 2004; Ohte et al. 2010; Pellerin et al. 2012; Piatek et al. 2005; Tsunogai et al. 2014). However, the contribution of nitrate from anthropogenic sources could be smaller in this area owing to lower population densities in the catchments (Table 1). Because a major portion of possible anthropogenic nitrate in the catchments must be occupied by $\mathrm{NO_3^-}_{\mathrm{re}}$ (Ohte et al. 2010), a lower $\mathrm{NO_3^-}_{\mathrm{re}}$ supply from anthropogenic sources in each catchment area could elevate the mixing ratio of unprocessed $\mathrm{NO_3^-}_{\mathrm{atm}}$ within the total nitrate pool even if absolute concentration of $\mathrm{NO_3^-}_{\mathrm{atm}}$ (C_{atm}) was uniform in the streams.

To determine the C_{atm} variability among the streams, the C_{atm} values estimated in this study were plotted as a function of population densities in Fig. 7(b). The C_{atm} was almost uniform at

2.3 ± 1.1 µmol L^{-1} irrespective of changes in the population density of each catchment area. However, a clear C_{total} enrichment trend was noted in accordance with the increase in population densities of the catchments (Fig. 7(a)). Similar C_{total} enrichment trends have been reported in previous studies (Ohte et al. 2010).

The northern streams such as Nos. 3, 4, and 5 were enriched in C_{atm}, showing C_{atm} annual average values of 5.3 ± 0.9, 2.9 ± 0.6, and 4.3 ± 0.8 µmol L^{-1}, respectively, and $\Delta^{17}O$ values of +3.1‰, +1.9‰, and +2.9‰, respectively. These results support the previous observation of the streams determined by using the $\delta^{18}O$ tracer. Similar C_{atm} enrichment of about 3 µmol L^{-1} or more, however, was also found in streams in other areas, such as Nos. 14 ($C_{atm} = 3.3 \pm 0.9$ µmol L^{-1}), 25 (3.2 ± 0.7 µmol L^{-1}), and 21 (4.2 ± 0.8 µmol L^{-1}), while showing lower $\Delta^{17}O$ values of +0.9‰, +1.5‰, and +2.0‰, respectively, thus showing low mixing ratios of unprocessed $NO_3^-{}_{atm}$ within total nitrate. We concluded that the difference in the addition of anthropogenic nitrate composed of $NO_3^-{}_{re}$ in the catchments was primarily responsible for the difference in the mixing ratio of unprocessed $NO_3^-{}_{atm}$ within the total nitrate pool, as well as C_{total} variation in accordance with the population densities of the catchment area as shown in Fig. 1. That is, a small contribution of anthropogenic nitrate in the catchments in the northern rivers was primarily responsible for the low C_{total} and thus the high mixing ratio of unprocessed $NO_3^-{}_{atm}$ within the total nitrate pool, or C_{atm}/C_{total} ratios, in the northern streams of the watershed.

Although the difference in the accumulation rate of snow between each catchment zone was not the major factor controlling the C_{atm}/C_{total} ratios, the concentrated release of $NO_3^-{}_{atm}$ stored in the snowpack during the melting seasons should be one of the important factors in determining the C_{atm} variation among the streams. Most of the C_{atm}-enriched streams, such as Nos. 3, 4, 5, 14, and 25, originated from forested catchment ~~in~~ high elevations of more than 800 m above sea level; thus, we can anticipate heavy snowpack in winter of each headwater. Moreover, the maximum C_{atm} values in these streams were found in March, which is the season of snowmelt (Fig. 5). On the contrary, most of the C_{atm}-depleted streams such as Nos. 29 (0.9 ± 0.3 µmol L^{-1}), 19 (0.8 ± 0.2 µmol L^{-1}), 23 (0.5 ± 0.2 µmol L^{-1}), and 30 (0.6 ± 0.2 µmol L^{-1}) originated from low elevations having urban and sub-urban catchment areas (Table 1). As a result, the concentrated release of stored $NO_3^-{}_{atm}$ in the snowpack to the forest floor in the catchment zone during the melting seasons is strongly responsible for the C_{atm}

enrichment for some of the streams, particularly that in the streams during March as presented in Fig. 1.

The only exception is stream No. 21, located in the southernmost part of the watershed, which showed a high annual average C_{atm} of 4.2 ± 0.8 μmol L^{-1}. This small stream originated from a low elevation of about 200 m having a small catchment area of 4 km^2. In addition, although the other C_{atm}-enriched streams showed the maximum C_{atm} in March, that in No. 21 was highest in August, showing extraordinarily high C_{atm} of more than 10 μmol L^{-1}. It is unlikely that the $NO_3^-{}_{atm}$ stored in the snowpack in winter was the major source of $NO_3^-{}_{atm}$ in this stream.

The catchment zone of stream No. 21 showed the highest population density within the catchments of the streams studied (Table 1). About one-third of the catchment includes residential areas. Artificial drainage systems in urban or residential areas and agricultural lands in humid temperate regions are usually designed to drain rainwater efficiently into streams (Takimoto et al. 1994). As a result, a significant portion of $NO_3^-{}_{atm}$ deposited into the catchment area was deposited onto paved surfaces and was then drained directly into the stream via storm sewers without penetrating the ground. Thus, no interaction occurred with soils, as presented in Fig. 1. Because biogeochemical interactions within soils are the major sink for $NO_3^-{}_{atm}$ and thus for ^{17}O anomalies of nitrate (Nakagawa et al. 2013; Tsunogai et al. 2014), the development of such sewage systems in urban/suburban areas is strongly responsible for the high C_{atm} in stream No. 21. Similar bypassing effects of $NO_3^-{}_{atm}$ from soil contacts by paved surfaces have been suggested in urban/suburban watersheds by using $\delta^{18}O$ values of nitrate as tracers (Burns et al. 2009; Kaushal et al. 2011). We further verified that the sewage systems in urban/suburban catchments changed the fate of the $NO_3^-{}_{atm}$ deposited onto land to some extent.

The observed uniform C_{atm} irrespective of population densities and headwater elevations shown in Fig. 7 implies that the influences of snow packs and paved surfaces were still minor in determining the C_{atm} values in the streams. Rather, the observed stable C_{atm} implies that most of $NO_3^-{}_{atm}$ in the streams had been stored in groundwater/subsurface runoff in the watershed having similar C_{atm} concentrations and then gushed to the surface at respective headwater zones of various elevations and various land uses as presented in Fig. 1.

When using the $\delta^{18}O$ tracer, it was difficult to determine the precise absolute concentration of $NO_3^-{}_{atm}$ (C_{atm}) in each stream water as presented in this study and to determine whether the absolute concentration of $NO_3^-{}_{atm}$ was stable among the streams. By using the $\Delta^{17}O$ values, however, we can determine the precise C_{atm} in each stream for each season; thus, we can clarify the fate of $NO_3^-{}_{atm}$.

3.7 Differences in outflows from inflows

The concentrations and $\delta^{15}N$, $\delta^{18}O$, and $\Delta^{17}O$ values of nitrate in the outflow (Seta River; No. 33) are also presented in Fig. 4. In a manner similar to the inflow streams (i.e. by using Eqs. (3) to (5)), we estimated the annual average concentration of total nitrate in the outflow river ($\overline{C}_{total}$) to be 13.3 μmol L^{-1}, the annual average $\delta^{15}N$ values ($\overline{\delta^{15}N}$) to be +13.1‰, the annual average $\delta^{18}O$ values ($\overline{\delta^{18}O}$) to be +1.5‰, and the annual average $\Delta^{17}O$ values ($\overline{\Delta^{17}O}$) to be +0.9‰, as presented in Fig. 4. Moreover, in a manner similar to that used for the inflow streams (i.e. by using Eqs. (2), (6), and (7)), we estimated the annual average concentration of $NO_3^-{}_{atm}$ in the outflow river ($\overline{C}_{atm}$) to be 0.4 ± 0.1 μmol L^{-1}, the annual average $\delta^{15}N_{re}$ values ($\overline{\delta^{15}N_{re}}$) to be +13.7 ± 0.2‰, and the annual average $\delta^{18}O_{re}$ values ($\overline{\delta^{18}O_{re}}$) to be −1.2 ± 0.6‰, as presented in Fig. 5. Similar to that for inflows, the $\Delta^{17}O$ values were typical for nitrate in the natural stream waters. The striking features of the outflow in comparison with the inflows were the depletions of both C_{total} and C_{atm} as well as the ^{15}N enrichment in the outflow compared with that in the inflow (Figs. 4 and 5). Because the denitrification/assimilation processes remove both nitrate and $NO_3^-{}_{atm}$ and preferentially consumes ^{14}N during the removal, the progress of denitrification/assimilation in the lake water column can be strongly responsible for the removal of both nitrate and $NO_3^-{}_{atm}$, as well as the ^{15}N enrichment of nitrate in the outflow compared with the inflow. If this were the case in Lake Biwa, the total nitrate efflux must have been smaller than the total nitrate influx. To quantitatively verify this hypothesis and to evaluate the influences of the stagnated flow ~~into~~ the lake on nitrate, we estimated the total influx through all of the inflow streams for nitrate and $NO_3^-{}_{atm}$, ΔN_{in}, and ΔA_{in}, respectively, and the total efflux for nitrate and $NO_3^-{}_{atm}$, ΔN_{out}, and ΔA_{out}, respectively, as well as the flow-weighted average $\delta^{15}N$, $\delta^{18}O$, and $\Delta^{17}O$ values of all inflows and outflows, to discuss their changes in the lake.

The ΔN_{in} and ΔA_{in} in each interval between the observation n and the next observation n + 1 (i.e. each season) and the flow-weighted average $\delta^{15}N$, $\delta^{18}O$, and $\Delta^{17}O$ values of the inflows ($\delta(n)$) during each interval between the observation n and the next observation n + 1 were determined by using the following equations:

Biogeosciences Discuss., doi:10.5194/bg-2015-627, 2016
Manuscript under review for journal Biogeosciences
Published: 18 January 2016

$$\alpha = \frac{Q_{in}}{\sum_i q_i}, \tag{9}$$

$$\Delta N_{in}(n) = \sum_i C_i \cdot f_i \cdot \Delta t_i \cdot \alpha, \tag{10}$$

$$\delta(n) = \frac{\sum_i \delta_i \cdot C_i \cdot f_i \cdot \Delta t_i}{\sum_i C_i \cdot f_i \cdot \Delta t_i}, \tag{11}$$

$$\Delta A_{in}(n) = \Delta N_{in}(n) \cdot \frac{\Delta^{17}O_{in}(n)}{\Delta^{17}O_{atm}}, \tag{12}$$

$$\Delta N_{in} = \sum_{n=1}^{4} \Delta N_{in}(n), \tag{13}$$

$$\Delta A_{in} = \sum_{n=1}^{4} \Delta A_{in}(n), \tag{14}$$

$$\delta = \frac{\sum_{n=1}^{4} \delta(n) \cdot \Delta N_{in}(n)}{\sum_{n=1}^{4} \Delta N_{in}(n)}, \tag{15}$$

where Q_{in} denotes the annual gross influx of water into the lake; C_i and δ_i denote the concentration and isotopic values ($\delta^{15}N$, $\delta^{18}O$, or $\Delta^{17}O$) of nitrate on each stream i during each observation n, respectively; f_i denotes the flow rate of each stream i during each observation n; and Δt_n denotes the time interval between the observation n and the next observation n + 1.

For Q_{in}, we used the annual influx of water estimated by Kunimatsu et al. (1995), in which the influx via streams and that via groundwater were included. To include the influx of nitrate via groundwater and the other minor streams not measured in this study during the calculations, we used the correction factor α in Eq. (9), whereby we assumed that both the average concentration and average isotopic compositions of the inflows determined in this study represented those of all inflows into the lake, while assuming an error range of 20% on α.

By using the aforementioned equations, we estimated the total influx of nitrate to the lake (ΔN_{in}) for each interval, together with the average $\delta^{15}N$, $\delta^{18}O$, and $\Delta^{17}O$ values of nitrate during each interval, as presented in Table 2. Moreover, by using the values of ΔN_{in} during each interval, as well as their $\delta^{15}N$, $\delta^{18}O$, and $\Delta^{17}O$ values, we estimated the total influx of $NO_3^-{}_{atm}$ to the lake (ΔA_{in}) and their average $\delta^{15}N_{re}$ and $\delta^{18}O_{re}$ values for each interval, as presented in Table 2, by using Eqs. (12), (6), and (7). Furthermore, we estimated the annual total influx and their annual average values, as shown in Table 2.

The estimated annual average Δ^{17}O value of inflows, +1.3‰, corresponded to the average mixing ratio of $NO_3^-{}_{atm}$ within total nitrate ~~was~~ 5.1 ± 0.5%. We concluded that about 5% of the total nitrate in the inflows originated directly from the atmosphere; therefore, the remainder of the nitrate was of remineralized origin ($NO_3^-{}_{re}$) likely produced through nitrification within the catchments, as discussed in section 3.4. In addition, we estimated the annual total influx of nitrate to the lake (ΔN_{in}) to be 199 ± 40 Mmol and that of $NO_3^-{}_{atm}$ (ΔA_{in}) to be 10.1 ± 2.0 Mmol.

Moreover, we estimated the total efflux of nitrate from the lake via the ~~outflows~~ (ΔN_{out}) and that of $NO_3^-{}_{atm}$ (ΔA_{in}) for each interval by using Eqs. (9) to (15) in which ΔN_{in} was replaced with ΔN_{out}, which is the gross efflux of nitrate from the lake via the streams and groundwater during the interval between the observation n and the next observation n + 1. Additionally, Q_{in} was replaced with Q_{out}, which is the annual gross efflux of water. To include the minor efflux of nitrate to ΔN_{out}, such as that via canals, we used the correction factor γ instead of α in Eqs. (9) and (10), whereby we assumed that both the concentration and isotopic compositions of the natural outflow determined for each season in this study represented all outflows. For Q_{out}, we used the annual efflux of water from Lake Biwa estimated by Kunimatsu et al. (1995), which included the efflux via a natural river (Seta River, No. 33) and that via canals.

Compared with the annual ΔN_{in}, 199 ± 40 Mmol, and annual ΔA_{in}, 10.1 ± 2.0 Mmol, both the annual ΔN_{out}, 67 ± 13 Mmol, and annual ΔA_{out}, 2.2 ± 0.4 Mmol, were significantly smaller by about 34% and 22%, respectively. Hence, Lake Biwa acts as a net sink for both nitrate and $NO_3^-{}_{atm}$, as previously implied from the ^{15}N enrichment in outflows. Considering that nitrate ~~occupied~~ about 70% of the total fixed N pool in the inflows and about 40% of the total fixed N pool in the ~~outflows~~ (Shiga_Prefecture 2015), Lake Biwa also acts as a net sink for fixed N. Similar results had been obtained in past studies that discussed fixed N input/output of the lake (Kunimatsu 1995; Tezuka 1985; Tezuka 1992; Yamada et al. 1996). As implied in the significant ^{15}N enrichment in the remineralized portion of nitrate ($\delta^{15}N_{re}$) in the outflow, +13.7 ± 0.2‰, compared to that in the inflow, +5.6 ± 0.3‰, partial removal of nitrate through either assimilation or denitrification to result in ^{15}N enrichment of residual nitrate is strongly responsible for the 8.1 ± 0.5‰ increase in $\delta^{15}N_{re}$, as well as the net removal of both nitrate and $NO_3^-{}_{atm}$ from the lake.

On the contrary, the $\delta^{18}O$ differences in the remineralized portion of nitrate ($\delta^{18}O_{re}$) between the inflows and outflows were significantly smaller than $\delta^{15}N_{re}$, at an annual average of only 1.6 ± 1.5‰ (Table 2). If nitrate in outflows is the residual of assimilation/denitrification in the lake, $\delta^{18}O_{re}$ should increase as well (Granger et al. 2008; Granger et al. 2004). The much smaller $\delta^{18}O_{re}$ difference implies that nitrate supplied directly from inflows occupied a small portion of nitrate in the outflows and that most of nitrate with high $\delta^{15}N$ values in the outflows had been produced through nitrification in the lake water column in which the fixed N had previously been enriched in ^{15}N. Isotopic fractionations during fixed N cycling in the lake such as denitrification or assimilation and the subsequent removal of ^{15}N-depleted organic N during sedimentation (Fig. 1) should be responsible for the ^{15}N enrichment of the total fixed N. That is, most of nitrate fed into the lake via the inflows had been removed at least once from the lake water column and been involved into the total fixed N cycling in the lake, in which the ^{15}N-enriched nitrate in the outflow had been produced (Fig. 1). The stagnation of flow in the lake encouraged primary production and thus the net removal of total fixed N through either denitrification or sedimentation, which resulted in ^{15}N enrichment of total fixed N pool compared with that in the inflows. Further studies on N cycling in the lake are needed to verify these results.

4 Concluding Remarks

In this study, we applied the $\Delta^{17}O$ tracer of nitrate to determine accurate and precise mixing ratios of unprocessed $NO_3^-{}_{atm}$ within the total nitrate value for more than 30 streams in the Lake Biwa watershed basin. Although the nitrate concentration changed from 12.7 to 106.2 µmol L^{-1} between the inflow streams and the mixing ratio of $NO_3^-{}_{atm}$ within total nitrate also changed from 1.8% to 11.8%, the absolute concentration of $NO_3^-{}_{atm}$ (C_{atm}) in each stream water was almost stable at 2.3 ± 1.1 µmol L^{-1} irrespective of the changes in population density and land use among the catchment areas. We concluded that changes in population density and land use in each catchment area had little impact on C_{atm}, and the total nitrate concentration was determined primarily by the extent of the additional $NO_3^-{}_{re}$ contribution mostly from anthropogenic sources. Relying on only the $\delta^{15}N$ and $\delta^{18}O$ tracers of nitrate, it was difficult to determine the precise C_{atm} in stream water and whether C_{atm} was uniform among the streams. By using the $\Delta^{17}O$ values, we can estimate accurate and precise C_{atm} in each stream for each season; thus, we can clarify the fate of $NO_3^-{}_{atm}$ deposited into the catchments.

Moreover, additional measurements of the $\Delta^{17}O$ values of nitrate together with $\delta^{15}N$ and $\delta^{18}O$ enabled us to exclude the contribution of $NO_3^-{}_{atm}$ from the determined $\delta^{15}N$ and $\delta^{18}O$ values and to use the corrected $\delta^{15}N$ and $\delta^{18}O$ values, $\delta^{15}N_{re}$ and $\delta^{18}O_{re}$, to evaluate the source and behaviour of $NO_3^-{}_{re}$ in each stream. Based on the correction, we successfully estimated the $\delta^{15}N$ and $\delta^{18}O$ values of $NO_3^-{}_{re}$ in the streams to be +4.4 ± 1.8‰ and −2.3 ± 0.9‰, respectively, for that produced through nitrification in naturally occurring soil organic matter and +9.2 ± 1.3‰ and −2.2 ± 1.1 ‰, respectively, for that supplied from anthropogenic sources, most of which had been occupied by sewage effluent. In addition, the low and uniform annual average $\delta^{18}O_{re}$ values of $NO_3^-{}_{re}$ in the streams implies that the denitrification in the riverbed sediments was minor in the streams.

Furthermore, we clarified the seasonal changes in the range of isotopic fractionation through partial nitrate removal via assimilation or denitrification by using the relationship between $\Delta^{17}O$ and $\delta^{18}O$ of nitrate in the streams. The changes were small in winter in all of the catchment area but large in summer in some catchments. Therefore, the relationship between $\Delta^{17}O$ and $\delta^{18}O$ of nitrate eluted from a catchment area is a powerful indicator for evaluating the biogeochemical nitrogen cycles within a catchment area, including the seasonal changes.

In summary, interpretations on the stable isotopic compositions of nitrate ($\delta^{15}N$ and $\delta^{18}O$) without $\Delta^{17}O$ values can be often misleading when assuming (1) $\delta^{18}O$ values simply reflect the mixing ratio of $NO_3^-{}_{atm}$ within total nitrate, (2) the mixing ratios of $NO_3^-{}_{atm}$ within the total NO_3^- is minimum for whole/specific samples studied, or (3) the mixing ratio of $NO_3^-{}_{atm}$ within total nitrate is uniform in whole/specific samples studied. In using the stable isotopic compositions of nitrate in freshwater environments to trace the source and fate of the nitrate, particularly the $\delta^{18}O$ value, determination of the $\Delta^{17}O$ values is essential.

Acknowledgements

We are grateful to Kosuke Ikeya, Hiroki Sakuma, Sho Minami, Kenta Ando, Shuichi Hara, Toshiyuki Matsushita, Takahiro Mihara, Teresa Fukuda, Yoshiumi Matsumoto, Rei Nakane, Lin Cheng, Yuuko Nakano, and other present and past members of the Biogeochemistry Group, Nagoya University, for their valuable support throughout this study. We thank Drs.

Shin-ichi Nakano, Tadatoshi Koitatabashi, Yukiko Goda, and other staff of the Center for Ecological Research, Kyoto University, for their valuable support during the field study in the Lake Biwa watershed basin. We also thank the members of the Machine Shop of Nagoya University Technical Center for their valuable support in developing the sampling and analytical devices used in this study. This work is supported by a Grant-in-Aid for Scientific Research from the Ministry of Education, Culture, Sports, Science, and Technology of Japan under grant numbers 24651002, 26241006, and 15H02804.

References

Alexander, B., M. G. Hastings, D. J. Allan, J. Dachas, J. A. Thornton, and S. A. Kunasek. 2009. Quantifying atmospheric nitrate formation pathways based on a global model of the oxygen isotopic composition (delta O-17) of atmospheric nitrate. Atmos. Chem. Phys. **9**: 5043-5056.

Aravena, R., M. L. Evans, and J. A. Cherry. 1993. Stable Isotopes of Oxygen and Nitrogen in Source Identification of Nitrate from Septic Systems. Groundwater **31**: 180-186.

Barnes, R., P. Raymond, and K. Casciotti. 2008. Dual isotope analyses indicate efficient processing of atmospheric nitrate by forested watersheds in the northeastern U.S. Biogeochemistry **90**: 15-27.

Barnes, R., and P. A. Raymond. 2010. Land-use controls on sources and processing of nitrate in small watersheds: insights from dual isotopic analysis. Ecol. Appl. **20**: 1961-1978.

Böttcher, J., O. Strebel, S. Voerkelius, and H. L. Schmidt. 1990. Using Isotope Fractionation of Nitrate Nitrogen and Nitrate Oxygen for Evaluation of Microbial Denitrification in a Sandy Aquifer. J. Hydrol. **114**: 413-424.

Buchwald, C., A. E. Santoro, M. R. Mcilvin, and K. L. Casciotti. 2012. Oxygen isotopic composition of nitrate and nitrite produced by nitrifying cocultures and natural marine assemblages. Limnol. Oceanogr. **57**: 1361-1375.

Burns, D. A., E. W. Boyer, E. M. Elliott, and C. Kendall. 2009. Sources and transformations of nitrate from streams draining varying land uses: Evidence from dual isotope analysis. Journal of Environmental Quality **38**: 1149-1159.

Burns, D. A., and C. Kendall. 2002. Analysis of δ^{15}N and δ^{18}O to differentiate NO_3^- sources in runoff at two watersheds in the Catskill Mountains of New York. Water Resour. Res. **38**: 1051, doi:10.1029/2001WR000292.

Campbell, D. H., C. Kendall, C. C. Y. Chang, S. R. Silva, and K. A. Tonnessen. 2002. Pathways for nitrate release from an alpine watershed: Determination using δ^{15}N and δ^{18}O. Water Resour. Res. **38**: 1052, doi:10.1029/2001WR000294.

Campbell, J. L., M. J. Mitchell, and B. Mayer. 2006. Isotopic assessment of NO_3^- and SO_4^{2-} mobility during winter in two adjacent watersheds in the Adirondack Mountains, New York. Journal of Geophysical Research **111**: G04007, doi: 04010.01029/02006JG000208.

Costa, A. W., G. Michalski, A. J. Schauer, B. Alexander, E. J. Steig, and P. B. Shepson. 2011. Analysis of atmospheric inputs of nitrate to a temperate forest ecosystem from Δ^{17}O isotope ratio measurements. Geophys. Res. Lett. **38**: L15805, doi: 10.1029/2011GL047539.

Curtis, C. J., C. D. Evans, C. L. Goodale, and T. H. E. Heaton. 2011. What have stable isotope studies revealed about the nature and mechanisms of N saturation and nitrate leaching from semi-natural catchments ? Ecosystems **14**: 1021-1037.

Dejwakh, N. R., T. Meixner, G. Michalski, and J. Mcintosh. 2012. Using ^{17}O to investigate nitrate sources and sinks in a semi-arid groundwater system. Environ. Sci. Technol. **46**: 745-751.

Durka, W., E.-D. Schulze, G. Gebauer, and S. Voerkeliust. 1994. Effects of forest decline on uptake and leaching of deposited nitrate determined from ^{15}N and ^{18}O measurements. Nature **372**: 765-767.

EANET. 2014. Data Report 2013. Network center for EANET (Acid Deposition Monitoring Network in East Asia), Nigata, Japan, 298 pp.

Fang, Y., K. Koba, A. Makabe, F. Zhu, S. Fan, X. Liu, and M. Yoh. 2012. Low delta O-18 Values of Nitrate Produced from Nitrification in Temperate Forest Soils. Environ. Sci. Technol. **46**: 8723-8730.

Granger, J., D. M. Sigman, M. F. Lehmann, and P. D. Tortell. 2008. Nitrogen and oxygen isotope fractionation during dissimilatory nitrate reduction by denitrifying bacteria. Limnol. Oceanogr. **53**: 2533-2545.

Granger, J., D. M. Sigman, J. A. Needoba, and P. J. Harrison. 2004. Coupled nitrogen and oxygen isotope fractionation of nitrate during assimilation by cultures of marine phytoplankton. Limnol. Oceanogr. **49**: 1763-1773.

Granger, J., D. M. Sigman, M. M. Rohde, M. T. Maldonado, and P. D. Tortell. 2010. N and O isotope effects during nitrate assimilation by unicellular prokaryotic and eukaryotic plankton cultures. Geochim. Cosmochim. Acta **74**: 1030-1040.

Hales, H. C., D. S. Ross, and A. Lini. 2007. Isotopic signature of nitrate in two contrasting watersheds of Brush Brook, Vermont, USA. Biogeochemistry **84**: 51-66.

Hirota, A., U. Tsunogai, D. D. Komatsu, and F. Nakagawa. 2010. Simultaneous determination of δ^{15}N and δ^{18}O of N2O and δ^{13}C of CH_4 in nanomolar quantities from a single water sample. Rapid Commun. Mass Spectrom. **24**: 1085-1092.

Hsieh, C. H., Y. Sakai, S. Ban, K. Ishikawa, T. Ishikawa, S. Ichise, N. Yamamura, and M. Kumagai. 2011. Eutrophication and warming effects on long-term variation of zooplankton in Lake Biwa. Biogeosciences **8**: 1383-1399.

Johannsen, A., K. Dähnke, and K. Emeis. 2008. Isotopic composition of nitrate in five German rivers discharging into the North Sea. Org. Geochem. **39**: 1678-1689.

Kaiser, J., M. G. Hastings, B. Z. Houlton, T. Röckmann, and D. M. Sigman. 2007. Triple oxygen isotope analysis of nitrate using the denitrifier method and thermal decomposition of N_2O. Anal. Chem. **79**: 599-607.

Kaushal, S. S., P. M. Groffman, L. E. Band, E. M. Elliott, C. A. Shields, and C. Kendall. 2011. Tracking nonpoint source nitrogen pollution in human-impacted watersheds. Environ. Sci. Technol. 45: 8225-8232.

Kendall, C. 1998. Tracing Nitrogen Sources and Cycling in Catchments, p. 519-576. In C. Kendall and J. J. McDonnell [eds.], Isotope Tracers in Catchment Hydrology. Elsevier Science B.V., Amsterdam, 839 p.

Kendall, C., D. H. Campbell, D. A. Burns, J. B. Schanley, S. R. Silva, and C. C. Y. Chang. 1995. Tracing sources of nitrate in snowmelt runoff using the oxygen and nitrogen isotopic compositions of nitrate, p. 339–347. Biogeochemistry of seasonally snow-covered catchments, Proceedings of a Boulder Symposium. IAHS Publication.

Komatsu, D. D., T. Ishimura, F. Nakagawa, and U. Tsunogai. 2008. Determination of the $^{15}N/^{14}N$, $^{17}O/^{16}O$, and $^{18}O/^{16}O$ ratios of nitrous oxide by using continuous-flow isotope-ratio mass spectrometry. Rapid Commun. Mass Spectrom. **22**: 1587-1596.

Konno, U., U. Tsunogai, D. D. Komatsu, S. Daita, F. Nakagawa, A.Tsuda, T. Matsui, Y.-J. Eum, and K. Suzuki. 2010. Determination of total N_2 fixation rates in the ocean taking into account both the particulate and filtrate fractions. Biogeosciences **7**: 2369-2377.

Kunasek, S. A., B. Alexander, E. J. Steig, M. G. Hastings, D. J. Gleason, and J. C. Jarvis. 2008. Measurements and modeling of Delta O-17 of nitrate in snowpits from Summit, Greenland. J. Geophys. Res. **113**: D24302, doi:10.1029/2008jd010103.

Kunimatsu, T. 1995. Mass balance of Lake Biwa. LBRI bulletin **12**: 68-73 (in Japanese).

Likens, G. E., F. H. Bormann, N. M. Johnson, D. W. Fisher, and R. S. Pierce. 1970. Effects of forest cutting and herbicide treatment on nutrient budgets in the Hubbard Brook watershed-ecosystem. Ecol. Monogr. **40**: 23-47.

Liu, T., F. Wang, G. Michalski, X. Xia, and S. Liu. 2013. Using N-15, O-17, and O-18 To Determine Nitrate Sources in the Yellow River, China. Environmental Science & Technology **47**: 13412-13421.

Lohse, K. A., J. Sanderman, and R. Amundson. 2013. Identifying sources and processes influencing nitrogen export to a small stream using dual isotopes of nitrate. Water Resour. Res. **49**: 5715–5731.

Mayer, B., S. M. Bollwerk, T. Mansfeldt, B. Huter, and J. Veizer. 2001. The oxygen isotope composition of nitrate generated by nitrification in acid forest floors. Geochim. Cosmochim. Acta **65**: 2743-2756.

Mayer, B., E. W. Boyer, C. Goodale, N. A. Jaworski, N. Van Breemen, R. W. Howarth, S. Seitzinger, G. Billen, L. J. Lajtha, M. Nosal, and K. Paustian. 2002. Sources of nitrate in rivers draining sixteen watersheds in the northeastern US: Isotopic constraints. Biogeochemistry **57**: 171-197.

Mcilvin, M. R., and M. A. Altabet. 2005. Chemical conversion of nitrate and nitrite to nitrous oxide for nitrogen and oxygen isotope analysis in freshwater and seawater. Anal. Chem. **77**: 5589-5595.

McIsaac, G. F., M. B. David, G. Z. Gertner, and D. A. Goolsby. 2001. Eutrophication: Nitrate flux in the Mississippi River. Nature **414**: 166-167.

Mcmahon, P. B., and J. K. Böhlke. 1996. Denitrification and mixing in a stream-aquifer system: Effects on nitrate loading to surface water. J. Hydrol. **186**: 105-128.

Michalski, G., T. Meixner, M. Fenn, L. Hernandez, A. Sirulnik, E. Allen, and M. Thiemens. 2004. Tracing Atmospheric Nitrate Deposition in a Complex Semiarid Ecosystem Using $\Delta^{17}O$. Environ. Sci. Technol. **38**: 2175-2181.

Michalski, G., J. Savarino, J. K. Böhlke, and M. Thiemens. 2002. Determination of the total oxygen isotopic composition of nitrate and the calibration of a $\Delta^{17}O$ nitrate reference material. Anal. Chem. **74**: 4989-4993.

Michalski, G., Z. Scott, M. Kabiling, and M. H. Thiemens. 2003. First measurements and modeling of $\Delta^{17}O$ in atmospheric nitrate. Geophys. Res. Lett. **30**: 1870, doi:10.1029/2003GL017015.

Miller, M. F. 2002. Isotopic fractionation and the quantification of ^{17}O anomalies in the oxygen three-isotope system: an appraisal and geochemical significance. Geochim. Cosmochim. Acta **66**: 1881-1889.

Morin, S., J. Erbland, J. Savarino, F. Domine, J. Bock, U. Friess, H.-W. Jacobi, H. Sihler, and J. M. F. Martins. 2012. An isotopic view on the connection between photolytic emissions of NO_X from the Arctic snowpack and its oxidation by reactive halogens. J. Geophys. Res. **117**: D00R08, doi:10.1029/2011JD016618.

Morin, S., J. Savarino, M. M. Frey, F. Domine, H. W. Jacobi, L. Kaleschke, and J. M. F. Martins. 2009. Comprehensive isotopic composition of atmospheric nitrate in the Atlantic Ocean boundary layer from 65 degrees S to 79 degrees N. J. Geophys. Res. **114**: D05303, doi: 10.1029/2008jd010696.

Morin, S., J. Savarino, M. M. Frey, N. Yan, S. Bekki, J. W. Bottenheim, and J. M. F. Martins. 2008. Tracing the origin and fate of NO_X in the Arctic atmosphere using stable isotopes in nitrate. Science **322**: 730-732.

Nakagawa, F., A. Suzuki, S. Daita, T. Ohyama, D. D. Komatsu, and U. Tsunogai. 2013. Tracing atmospheric nitrate in groundwater using triple oxygen isotopes: Evaluation based on bottled drinking water. Biogeosciences **10**: 3547-3558.

Nestler, A., M. Berglund, F. Accoe, S. Duta, D. Xue, P. Boeckx, and P. Taylor. 2011. Isotopes for improved management of nitrate pollution in aqueous resources: review of surface water field studies. Environmental Science and Pollution Research 18: 519-533.

Ohte, N. 2013. Tracing sources and pathways of dissolved nitrate in forest and river ecosystems using high-resolution isotopic techniques: a review. Ecol. Res. **28**: 749-757.

Ohte, N., S. D. Sebestyen, J. B. Shanley, D. H. Doctor, C. Kendall, S. D. Wankel, and E. W. Boyer. 2004. Tracing sources of nitrate in snowmelt runoff using a high-resolution isotopic technique. Geophys. Res. Lett. **31**: L21506, doi:10.1029/2004GL020908.

Ohte, N., I. Tayasu, A. Kohzu, C. Yoshimizu, K. Osaka, A. Makabe, K. Koba, N. Yoshida, and T. Nagata. 2010. Spatial distribution of nitrate sources of rivers in the Lake Biwa watershed, Japan: Controlling factors revealed by nitrogen and oxygen isotope values. Water Resour. Res. **46**: W07505, doi:10.1029/2009wr007871.

Paerl, H. W. 2009. Controlling eutrophication along the freshwater–marine continuum: Dual nutrient (N and P) reductions are essential. Estuar. Coasts **32**: 593-601.

Pellerin, B., J. Saraceno, J. Shanley, S. Sebestyen, G. Aiken, W. Wollheim, and B. Bergamaschi. 2012. Taking the pulse of snowmelt: in situ sensors reveal seasonal, event and diurnal patterns of nitrate and dissolved organic matter variability in an upland forest stream. Biogeochemistry **108**: 183-198.

Piatek, K. B., M. J. Mitchell, S. R. Silva, and C. Kendall. 2005. Sources of nitrate in snowmelt discharge: evidence from water chemistry and stable isotopes of nitrate. Water Air Soil Poll. **165**: 13-35.

Riha, K. M., G. Michalski, E. L. Gallo, K. A. Lohse, P. D. Brooks, and T. Meixner. 2014. High Atmospheric Nitrate Inputs and Nitrogen Turnover in Semi-arid Urban Catchments. Ecosystems **17**: 1309-1325.

Rose, L. A., E. M. Elliott, and M. B. Adams. 2015. Triple Nitrate Isotopes Indicate Differing Nitrate Source Contributions to Streams Across a Nitrogen Saturation Gradient. Ecosystems doi:10.1007/s10021-015-9891-8.

Savarino, J., S. Morin, J. Erbland, F. Grannec, M. D. Patey, W. Vicars, B. Alexander, and E. P. Achterberg. 2013. Isotopic composition of atmospheric nitrate in a tropical marine boundary layer. Proc. Natl. Aca. Sci. USA **110**: 17668-17673.

Shiga Prefecture. 2015. Annual Report on the Environment in Shiga (FY 2013), Appendix. Shiga prefecture, Japan, 332 pp (in Japanese).

Silva, S. R., P. B. Ging, R. W. Lee, J. C. Ebbert, A. J. Tesoriero, and E. L. Inkpen. 2002. Forensic spplications of nitrogen and oxygen isotopes in tracing nitrate sources in urban environments. Environ. Forensics 3: 125-130.

Spoelstra, J., S. L. Schiff, P. W. Hazlett, D. S. Jeffries, and R. G. Semkin. 2007. The isotopic composition of nitrate produced from nitrification in a hardwood forest floor. Geochim. Cosmochim. Acta **71**: 3757-3771.

Swank, W. T., J. M. Vose, and K. J. Elliott. 2001. Long-term hydrologic and water quality responses following commercial clearcutting of mixed hardwoods on a southern Appalachian catchment. Forest Ecol. Manag. **143**: 163-178.

Takimoto, H., T. Tanaka, and H. Horino. 1994. Does forest conserve runoff discharge during drought ? Trans. Jpn. Soc. Irrig. Drain. Reclam. Eng. **170**: 75-81.

Tezuka, Y. 1985. C:N:P Ratios of Seston in Lake Biwa as Indicators of Nutrient Deficiency in Phytoplankton and Decomposition Process of Hypolimnetic Particulate Matter. Jap. J. Limnol. **46**: 239-246.

---. 1992. Recent Trend in the Eutrophication of the North Basin of Lake Biwa. Jap. J. Limnol. **53**: 139-144.

Thibodeau, B., J.-F. Hélie, and M. F. Lehmann. 2013. Variations of the nitrate isotopic composition in the St. Lawrence River caused by seasonal changes in atmospheric nitrogen inputs. Biogeochemistry **115**: 287-298.

Tobari, Y., K. Koba, K. Fukushima, N. Tokuchi, N. Ohte, R. Tateno, S. Toyoda, T. Yoshioka, and N. Yoshida. 2010. Contribution of atmospheric nitrate to stream-water nitrate in Japanese coniferous forests revealed by the oxygen isotope ratio of nitrate. Rapid Commun. Mass Spectrom. **24**: 1281-1286.

Tsunogai, U., S. Daita, D. D. Komatsu, F. Nakagawa, and A. Tanaka. 2011. Quantifying nitrate dynamics in an oligotrophic lake using $\Delta^{17}O$. Biogeosciences **8**: 687-702.

Tsunogai, U., T. Kido, A. Hirota, S. B. Ohkubo, D. D. Komatsu, and F. Nakagawa. 2008. Sensitive determinations of stable nitrogen isotopic composition of organic nitrogen through chemical conversion into N_2O. Rapid Commun. Mass Spectrom. **22**: 345-354.

Tsunogai, U., D. D. Komatsu, S. Daita, G. A. Kazemi, F. Nakagawa, I. Noguchi, and J. Zhang. 2010. Tracing the fate of atmospheric nitrate deposited onto a forest ecosystem in eastern Asia using Δ^{17}O. Atmos. Chem. Phys. **10**: 1809-1820.

Tsunogai, U., D. D. Komatsu, T. Ohyama, A. Suzuki, F. Nakagawa, I. Noguchi, K. Takagi, M. Nomura, K. Fukuzawa, and H. Shibata. 2014. Quantifying the effects of clear-cutting and strip-cutting on nitrate dynamics in a forested watershed using triple oxygen isotopes as tracers. Biogeosciences **11**: 5411-5424.

Wankel, S. D., C. Kendall, C. A. Francis, and A. Paytan. 2006. Nitrogen sources and cycling in the San Francisco Bay Estuary: A nitrate dual isotopic composition approach. Limnol. Oceanogr. **51**: 1654-1664.

Widory, D., E. Petelet-Giraud, P. Négrel, and B. Ladouche. 2005. Tracking the Sources of Nitrate in Groundwater Using Coupled Nitrogen and Boron Isotopes: A Synthesis. Environmental Science & Technology **39**: 539–548.

Williard, K. W. J., D. R. Dewalle, P. J. Edwards, and W. E. Sharpe. 2001. ^{18}O isotopic separation of stream nitrate sources in mid-Appalachian forested watersheds. J. Hydrol. **252**: 174–188.

Xue, D. M., J. Botte, B. De Baets, F. Accoe, A. Nestler, P. Taylor, O. Van Cleemput, M. Berglund, and P. Boeckx. 2009. Present limitations and future prospects of stable isotope methods for nitrate source identification in surface- and groundwater. Water Res. **43**: 1159-1170.

Yamada, Y., T. Ueda, and E. Wada. 1996. Distribution of Carbon and Nitrogen Isotope Ratios in the Yodo River Watershed. Jap. J. Limnol. **57**: 467-477.

Yamazaki, A., T. Watanabe, and U. Tsunogai. 2011. Nitrogen isotopes of organic nitrogen in reef coral skeletons as a proxy of tropical nutrient dynamics. Geophys. Res. Lett. **38**: L19605, doi:10.1029/2011GL049053.

Yue, F.-J., S.-L. Li, Z.-Q. Zhao, and J. Hu. 2013. Using dual isotopes to evaluate sources and transformation of nitrogen in the Liao River, northeast China. Appl. Geochem. **36**: 1-9.

Zeng, H., and J. Wu. 2015. Tracing the Nitrate Sources of the Yili River in the Taihu LakeWatershed: A Dual Isotope Approach. Water **7**: 188-201.

Table 1 List of studied streams.

No.	Name	Loc.[#]	Basin Area[*] (km^2)	Population Density[*] (km^{-2})	Residential[*] (%)	No.	Name	Loc.[#]	Basin Area[*] (km^2)	Population Density[*] (km^{-2})	Residential[*] (%)
Inflow											
31	Tenjin	West	10	539	7.3	14	Seri	East	74	462	8.1
30	Mano	West	23	1048	15.6	15	Inukami	East	102	109	2.8
29	Wani	West	17	186	5.4	16	Ajiki	East	15	1002	20.1
28	U	West	7	66	0.8	17	Uso	East	84	411	11.0
1	Kamo	West	47	89	1.2	18	Bunroku	East	14	595	11.7
2	Ado	West	306	27	0.7	19	Nomazu	East	7	758	20.2
3	Ishida	North	60	84	2.0	20	Echi	East	211	110	2.5
4	Momose	North	13	65	0.6	27	Hino	South	226	338	8.4
5	Chinai	North	51	44	1.8	26	Yanomune	South	42	859	15.7
6	Ohura	North	39	98	2.7	25	Yasu	South	391	324	6.5
7	Oh	North	20	55	1.6	24	Yamaga	South	6	2540	33.7
8	Yogo	North	7	141	3.4	23	Sakai	South	2	979	27.7
9	Chonoki	North	10	412	13.5	22	Hayama	South	34	2048	29.7
10	Ta	North	36	301	9.6	34	Kusatsu	South	48	370	30.6
11	Ane	North	372	61	1.7	21	Nagaso	South	4	3174	31.4
12	Yone	North	15	2047	34.5	32	Fujinoki	South	4	1805	20.8
13	Amano	North	111	226	5.8						
						Outflow					
						33	Seta	South	3848	323	–

[#] Category of location classified by Ohte et al. (2010).

[*] Data source: Ohte et al. (2010).

Table 2 Estimated gross influx/efflux of total nitrate (ΔN) and atmospheric nitrate (ΔA) via inflows/outflows during each observation interval, together with the average $\delta^{15}N$, $\delta^{18}O$, and $\Delta^{17}O$ values of total nitrate and remineralized portions of nitrate ($\delta^{15}N_{re}$ and $\delta^{18}O_{re}$) in the inflows/outflows during each interval.

	Spring (n=1 to 2)	Summer (n=2 to 3)	Autumn (n=3 to 4)	Winter (n=4 to 5)	Annual (n=1 to 5)
Duration (days)	94	49	77	145	365
Inflow					
ΔN_{in} (10^6 mol)	69 ± 14	3 ± 1	13 ± 3	114 ± 2 3	199 ± 40
ΔA_{in} (10^6 mol)	6.4 ± 1.3	0.1	0.8 ± 0.2	2.8 ± 0.6	10.1 ± 2.0
$10^3\ \delta^{15}N$	+4.0	+6.8	+5.6	+5.6	+5.1
$10^3\ \delta^{18}O$	+6.1	–0.8	+3.3	–1.5	+1.4
$10^3\ \Delta^{17}O$	+2.5	+0.8	+1.7	+0.6	+1.3
$10^3\ \delta^{15}N_{re}$	+4.8 ± 0.7	+7.1 ± 0.2	+6.3 ± 0.5	+5.9 ± 0.2	+5.6 ± 0.3
$10^3\ \delta^{18}O_{re}$	−1.5 ± 1.8	−3.2 ± 0.5	−2.0 ± 1.2	−3.5 ± 0.4	−2.8 ± 0.9
Outflow					
ΔN_{out} (10^6 mol)	24 ± 5	6 ± 1	5 ± 1	32 ± 6	67 ± 13
ΔA_{out} (10^6 mol)	1.4 ± 0.1	0.1	0.2	0.4 ± 0.1	2.2 ± 0.4
$10^3\ \delta^{15}N$	+7.3	+11.4	+10.4	+18.0	+13.1
$10^3\ \delta^{18}O$	+3.4	+4.8	+3.0	–0.7	+1.5
$10^3\ \Delta^{17}O$	+1.6	+0.4	+1.4	+0.4	+0.9
$10^3\ \delta^{15}N_{re}$	+8.1 ± 0.4	+11.7 ± 0.1	+11.2 ± 0.4	+18.3 ± 0.1	+13.7 ± 0.2
$10^3\ \delta^{18}O_{re}$	−1.5 ± 1.1	+3.6 ± 0.3	−1.2 ± 0.9	−1.9 ± 0.2	−1.2 ± 0.6

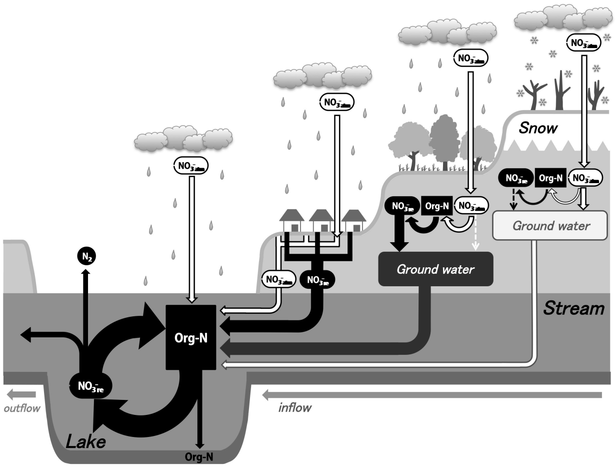

Figure 1. Schematic diagram showing the biological processing of atmospheric nitrate ($NO_3^-{}_{atm}$) and remineralized nitrate ($NO_3^-{}_{re}$) in the watershed with catchments of varying land uses and in the lake water column.

Biogeosciences Discuss., doi:10.5194/bg-2015-627, 2016
Manuscript under review for journal Biogeosciences
Published: 18 January 2016

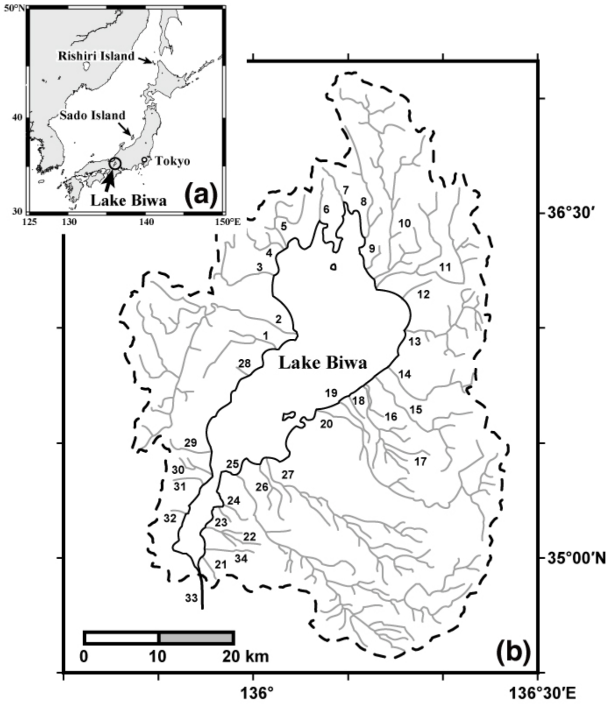

Figure 2. (a) Map showing the location of Lake Biwa watershed basin in Japan and Sado Island, where the Sado-seki National Acid Rain Monitoring Station is located. (b) Map showing the boundary of the Lake Biwa watershed basin (dashed line) and the locations of the inflows (represented by numbers) and outflow (Seta River, No. 33) studied in this paper (modified from Ohte et al. 2010).

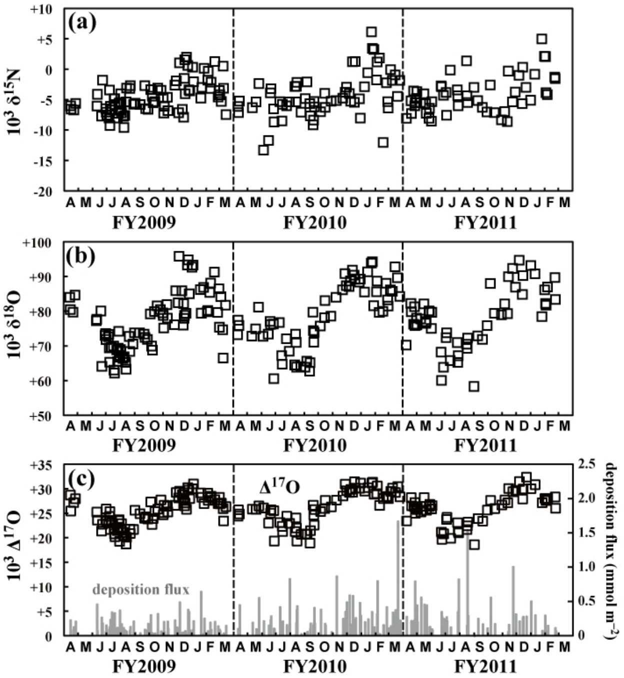

Figure 3. Temporal variations in the values of (a) $\delta^{15}N$, (b) $\delta^{18}O$, and (c) $\Delta^{17}O$ of nitrate in wet deposition recorded at the Sado-seki National Acid Rain Monitoring Station. Total deposition flux of nitrate during each rain event was also presented (c).

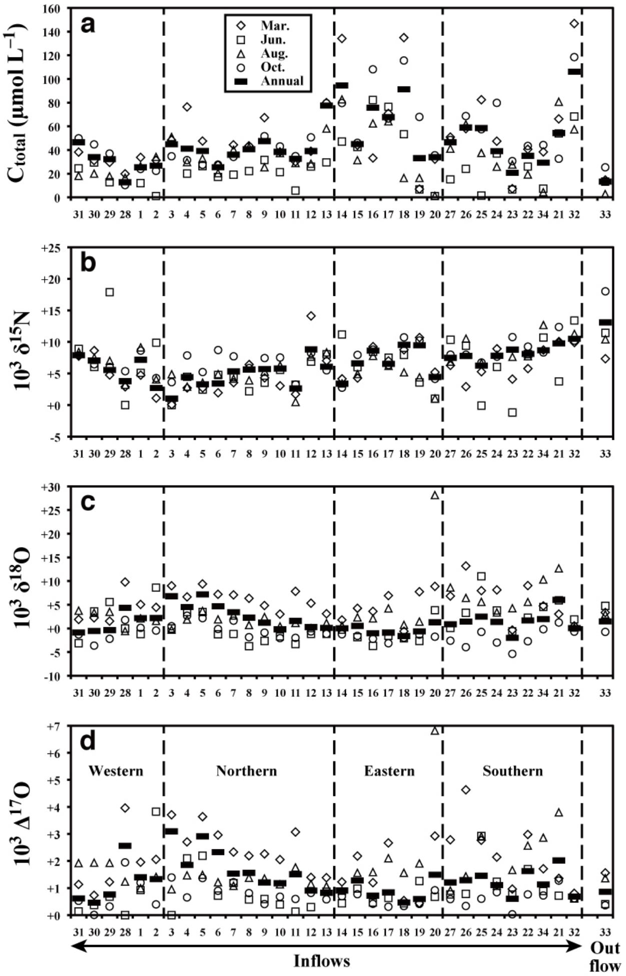

Figure 4. Distribution of (a) total concentrations, (b) $\delta^{15}N$, (c) $\delta^{18}O$, and (d) $\Delta^{17}O$ for nitrate in inflow streams showing various station numbers and the outflow at station No. 33 in Lake Biwa watershed in March (diamonds), June (squares), August (triangles), and October (circles) 2013 together with the annual averages for each river (black bars).

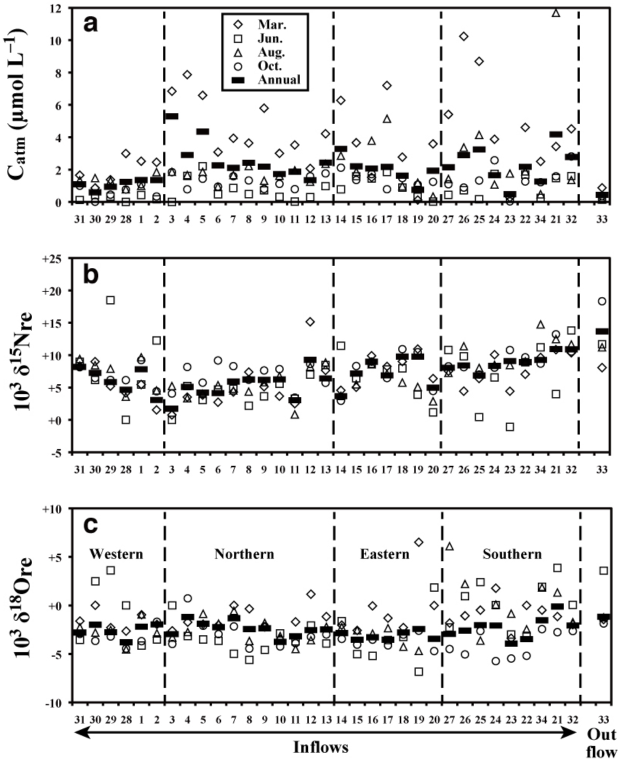

Figure 5. Distribution of concentrations of (a) atmospheric nitrate and (b) δ^{15}N and (c) δ^{18}O for remineralized nitrate ($\delta^{15}N_{re}$ and $\delta^{18}O_{re}$, respectively) in inflow streams shown by various station numbers and the outflow at station No. 33 of Lake Biwa watershed in March (diamonds), June (squares), August (triangles), and October (circles) 2013 together with the annual averages for each river (black bars).

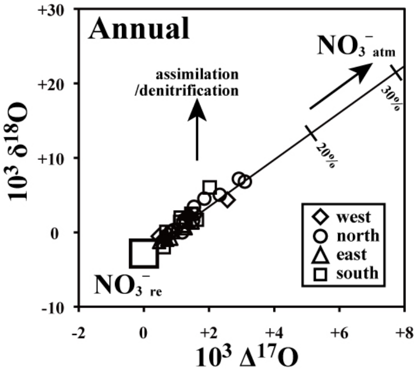

Figure 6. Relationship of the annual average values of $\Delta^{17}O$ and $\delta^{18}O$ of NO_3^- in the inflow streams. The symbols represent the location of each river (west: diamonds; north: circles; east: triangles; south: squares). A hypothetical mixing line between atmospheric nitrate ($NO_3^-{}_{atm}$) and remineralized nitrate ($NO_3^-{}_{re}$) is shown together with the end member value of $NO_3^-{}_{re}$ (large white square) and the 20% and 30% mixing ratios of $NO_3^-{}_{atm}$ on the line.

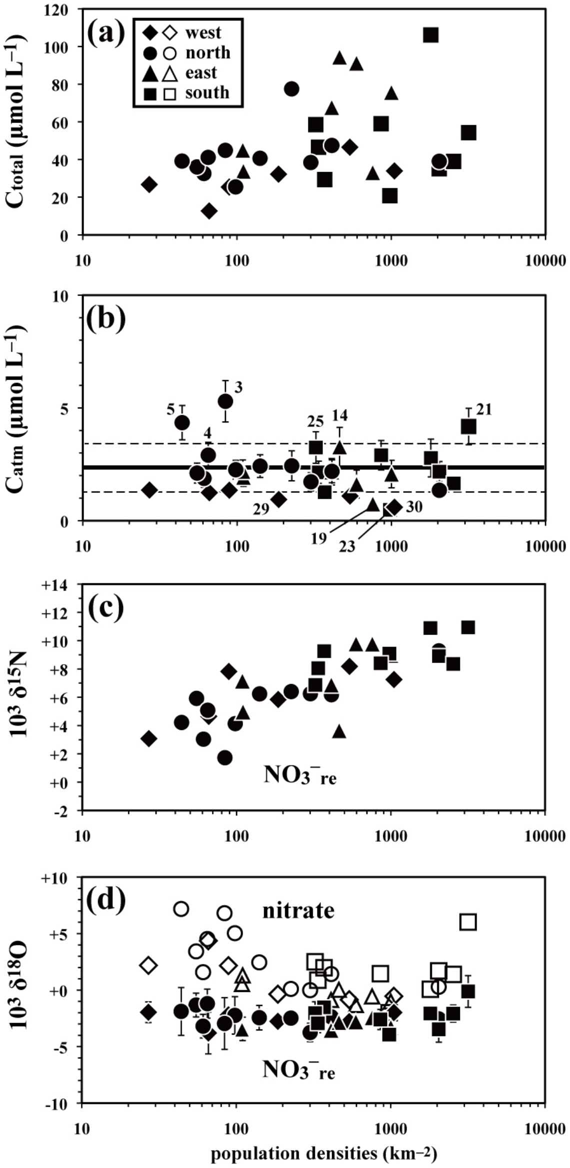

Figure 7. Annual average concentration of (a) nitrate (C_{total}) and that of (b) $NO_3^-{}_{atm}$ (C_{atm}) in each inflow stream plotted as a function of the population density in each catchment, together with (c) the annual average value of $\delta^{15}N$ and (d) that of $\delta^{18}O$ for remineralized NO_3^- ($NO_3^-{}_{re}$). (d) The annual average $\delta^{18}O$ values of nitrate are also presented. The symbols represent the location of each river (west: diamonds; north: circles; east: triangles; south: squares). The uncertainties are presented only for those larger than the symbols.

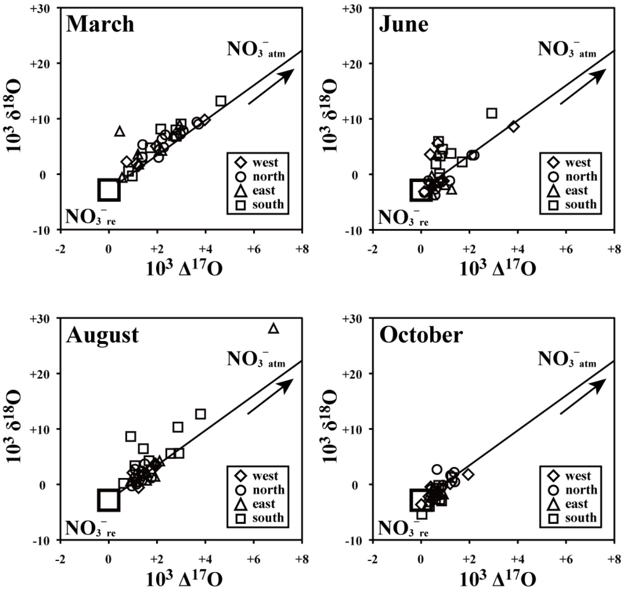

Figure 8. Temporal changes in the relationship between the values of $\Delta^{17}O$ and $\delta^{18}O$ of total nitrate in the stream water. The symbols are the same as those in Figure 6. A hypothetical mixing line between atmospheric nitrate ($NO_3^-{}_{atm}$) and remineralized nitrate ($NO_3^-{}_{re}$) is also shown together with the end member value of $NO_3^-{}_{re}$ (large white square).